The Electrical Properties of Interfacial Water and Their Applications

Chien-Chang Kurt Kung

A dissertation submitted in partial fulfillment of the requirements for the degree of

Doctor of Philosophy

University of Washington
2015

Reading Committee:

Gerald H. Pollack, Chair

Karl Böhringer

Werner Karminsky

Alexander Mamishev

Program Authorized to Offer Degree: Electrical Engineering and Nanotechnology

University of Washington

Abstract

The Electrical Properties of Interfacial Water and Their Application

Chien-Chang Kung

Chair of the Supervisory Committee:
Dr. Gerald H. Pollack
Bioengineering

The electrical properties of interfacial water [1] were explored to determine their capacity to deliver energy for practical applications. Interfacial water was created in the standard way, next to a sheet of hydrophilic membrane placed in a water-filled chamber. All measurements were done under room temperature and standard laboratory conditions in the absence of any external energy or light source, except for the ubiquitous infrared emissions from the normal environment [2]. Additionally, we designed and investigated different microelectrode systems to upscale the harvest of energy from interfacial water.

Studies were also extended to understand the biological effects of atmospheric ions on interfacial water. Positive atmospheric ions were created by the coronal discharge technique. Using micropipette electrodes, the distribution of electrical potential in the interfacial water was measured and it was observed that beyond a threshold, positive ions diminished the magnitude of the negative electrical potential in the interfacial water. Additionally, positive ions produced by an air conditioner were observed to generate similar effects. In fact, sometimes the positive ion effect from air conditioner was strong enough to destroy the structure of interfacial water by turning its potential decidedly positive. Thus, positive air ions can compromise interfacial water negativity, and may well explain the known negative impact of positive ions on health ([3]-[4]).

To my family.

TABLE OF CONTENTS

LIST OF FIGURES

LIST OF TABLES

ACKNOWLEDGEMENTS

I would first like to thank my advisor, Jerry Pollack. Without his mentorship and support, I wouldn't be able to accomplish my work and finish my Ph.D. He is my mentor not only in science and research, but also in life. I am constantly amazed by his enthusiasm and energy from time to time. It inspires me, and has a great positive influence on my whole Ph.D. career.

I am very fortunate to work with a group of talented colleagues and friends in the past six years. With their help, we have accomplished something that was previous considered impossible. It is truly my honor to be able to work with them.

Last but not the least, I would like to thank my parents, Ming Kung and Li-hua Pan. With their unconditional love and support, I have the chance to follow my dream and to be myself.

Chapter 1. INTRODUCTION

1.1 INTERFACIAL WATER

Water is an essential element for life and also one of the most abundant substances on earth. In fact, over 70% area on earth is covered by water. The majority of our bodies is made up of water. Water, however, is never alone and is profoundly affected by all kinds of surface. Practically any surface that touches water will have an effect: the container, suspended particles, or even dissolved molecules.

Well known for over a hundred years, interfacial water is often called as the “unstirred layer” by biologists. Since most biological materials are hydrophilic, interfacial water would be expected to exist nearly everywhere in biological environments. In 1949, Henniker cited more than a hundred published studies confirming the long-range effect of various surfaces on many liquids, including water [5]. Recently, we discovered another long-range effect of water found adjacent to the hydrophilic surfaces [1], where it formed a unique, extensive structure with different physico-chemical properties different from the bulk water. As a consequence of such unique structure, it generally stored net negative charge. The ubiquity of this charged entity, involved in all major cellular processes [6], implies that the interfacial water might be a common target for various biological studies.

Moreover, based on the unique charge separation phenomenon observed between interfacial water and bulk water, many practical applications can be developed. One of the most important technologies would be extracting the electrical energy from the structured interfacial water.

1.2 HYDROPHILIC SURFACES

Many tested materials were theorized to generate the structured interfacial water. Materials include biological cells, muscles, hydrogels, cellulose and etc. The two main testing methodologies were microsphere free zone test and electrical potential test. During the formation of interfacial water, there is an exclusion of the small particles, microspheres for example, within the interfacial region. This region of water usually extends from tens to hundreds microns from the surface and as a consequence, stores net negative charge. Therefore, we can use these two methodologies to test if the structured interfacial water is formed.

Among many materials that are capable to form structured interfacial water, we use mostly the artificial polymer, Nafion[7]. The main reason we choose Nafion is due to the consistency of its ability to generate stable structured interfacial water. Nafion ionomers were designed and developed by the E. I. Dupont company. These materials are generated by copolymerization of a perfluorinated vinyl ether co-monomer with tetrafluoroethylene (TFE), and TFE is the basic unit of the well-known material, Teflon. In other words, the chemical structure of Nafion (Fig. 1.1) has Teflon backbone with sulfonic acid functional group at the end of each monomer.

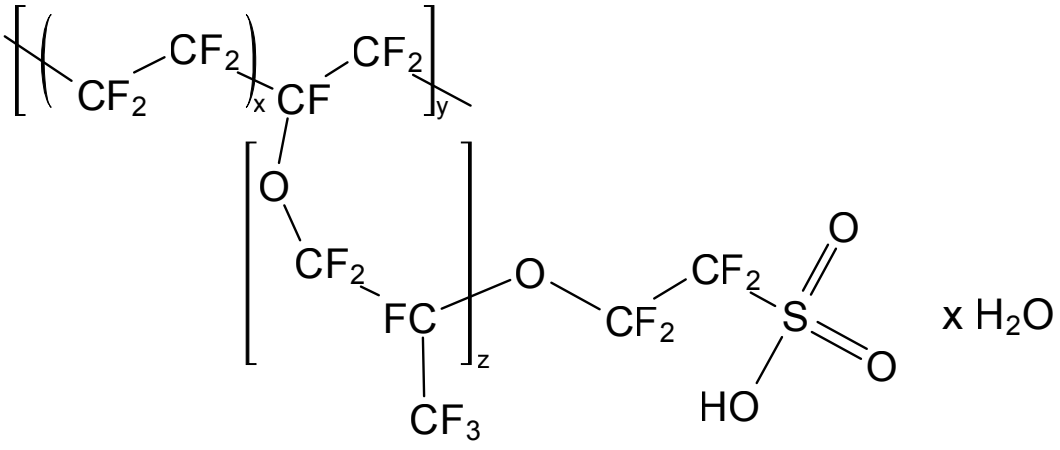

Figure 1. Chemical structure of Nafion.

1.3 ENGINEERING APPLICATION - ENERGY HARVESTING

Satisfying the world's energy needs is a demanding endeavor. Presently, fossil fuels are responsible for supplying the bulk of these worldwide needs. However, fossil fuel supplies are finite, their consumption often has adverse environmental effects, their cost widely variable and somewhat unpredictable, and independence from them is long considered to be politically advantageous.

Renewable energy technology is one of the most important topics in applied engineering, with a high level of potential societal impact. While renewable energy sources vary widely, solar energy is the most popular one. The photovoltaic cell is one of the common technologies that allow us to use the energy from sun; however, it does not work without direct sunlight exposure. As a matter of fact, no current existing renewable energy technology can deliver continuous stable power. Regulating the unpredictable power generation often requires an extra rechargeable battery device. This not only increases the cost but also makes the green energy less green. Here we propose a novel renewable energy technology using light, but not necessarily direct sunlight to generate electricity. The photovoltaic-like medium is water.

As described earlier, recent studies conclusively demonstrate that water forms a unique crystalline structure adjacent to many hydrophilic materials. This crystalline structure causes charge separation between the interfacial water and bulk water [1]. Therefore, the practical outcome from this charge separation is the production of electrical energy. From our previous work, we have learned that weak infrared light can increase the size of structured interfacial water dramatically [2]. Our preliminary experiments also indicate infrared light is the major contributor to the charge separation in water. In other words, water can be used as a medium to convert the infrared light into electricity.

1.4 BIOLOGICAL APPLICATION – EFFECT OF AIR IONS ON HEALTH

More than 200 years ago, Franklin [8] and d'Alibard [9] both, independently discovered atmospheric electricity. Soon after that, many scientists studied the biological effects arising from both positive and negative air ions [10]. Such effects include the killing of bacteria [11], changing the growth rate of plants and insects [12],[13], and various physiological and behavioral changes in animals and humans [14],[15]. To date, however, there is still no agreement on the mechanism of the biological effects of charged air ions.

Interfacial water exists nearly everywhere in biological environments. This charged entity is involved in all major cellular processes [6], implying that it might be a common target for the known effects of atmospheric electricity. We produced air ions using coronal discharge [16], and studied the effects of those positive air ions on the electrical properties of interfacial water. Clear effects were found. Based on the results obtained, we propose a new way to explain the biological effects of air ions.

Chapter 2. ENERGY HARVESTING FROM INTERFACIAL WATER

2.1 MATERIALS AND METHODS

Nafion 117 perfluorinated membranes (0.007 in. thick, Aldrich) were used as the hydrophilic surface. Before use, the Nafion membrane was immersed in deionized water for 10 minutes at room temperature. Besides Nafion, other hydrophilic materials such as polyacrylic acid (PAA) gel, polyvinyl acetate (PVA) gel and cellulose acetate [17] also have been demonstrated to produce similar effects. However, to the best of our knowledge, Nafion has the most stable and highest performance for energy harvesting applications.

Deionized water was obtained from a NANOpure Diamond ultrapure water system. The purity of water from this system was certified by a resistivity value up to 18.2 MΩ · cm, which exceeded ASTM, CAP, and NCCLS type I water requirements. In addition, the deionized water was passed through a 0.2-μm hollow fiber filter to ensure bacteria- and particle-free water before filling the glass chamber (dimensions -7 × 4.5 × 2.5 cm) to a consistent height of 1 cm for all experiments.

The general experimental setup and the configuration of the charge separation between interfacial water and bulk water are shown in Fig. 2.1 Except for the studies on the potential profile over distance measurements, the probe microelectrode usually remained on the Nafion surface. The reference electrode was placed remotely in the bulk water region. A passive resistor placed in parallel with the electrometer worked as a load resistor. By changing the resistance of this resistor, we could obtain the most important information, current-voltage (IV) curve, for the system power output. In this study, three different kinds of electrode systems were explored.

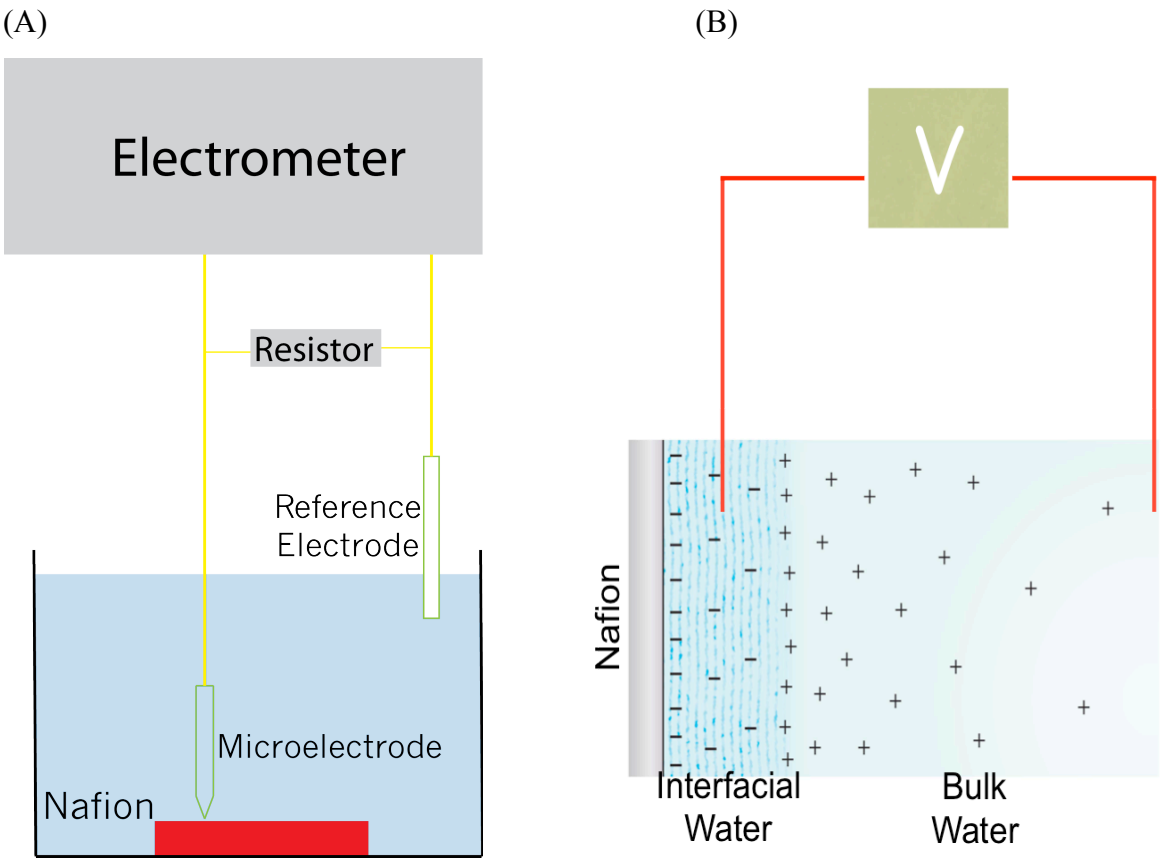

Figure 2.1. (A) Simplified diagram of experimental setup for measuring the potential and current from interfacial water. (B) Simplified diagram showing the configuration of charge separation between interfacial water and bulk water.

2.2 MICROPIPETTE ELECTRODE SYSTEM

2.2.1 *Single Pair of Micropipette Electrodes*

Initially, we started with standard glass microelectrodes pulled by a micropipette puller (P-87, Sutter Instrument) and filled with 3M KCl. Diameters of the microelectrode tips were less than 1 µm. To check for electrode quality, the probing and reference electrodes were immersed in 3M KCl prior to each experiment. The potential difference between the two electrodes was negligibly small in 3M KCl, and could be neglected.

However, in deionized water, a DC offset almost always appeared due to the deionized water's poor conductivity. The DC offset could be anywhere between -20 mV to +20 mV. To measure the electrical potential distribution in the water in the vicinity of Nafion, we used a motor to advance the probe electrode. The motor was controlled by software written in Labview, and had a spatial resolution of 1.25 μm.

We started with the 3M KCl micropipette electrode system to explore the fundamental electrical properties of interfacial water. For energy harvesting purpose, we placed the probe electrode as close to the Nafion surface as possible through all experiments.

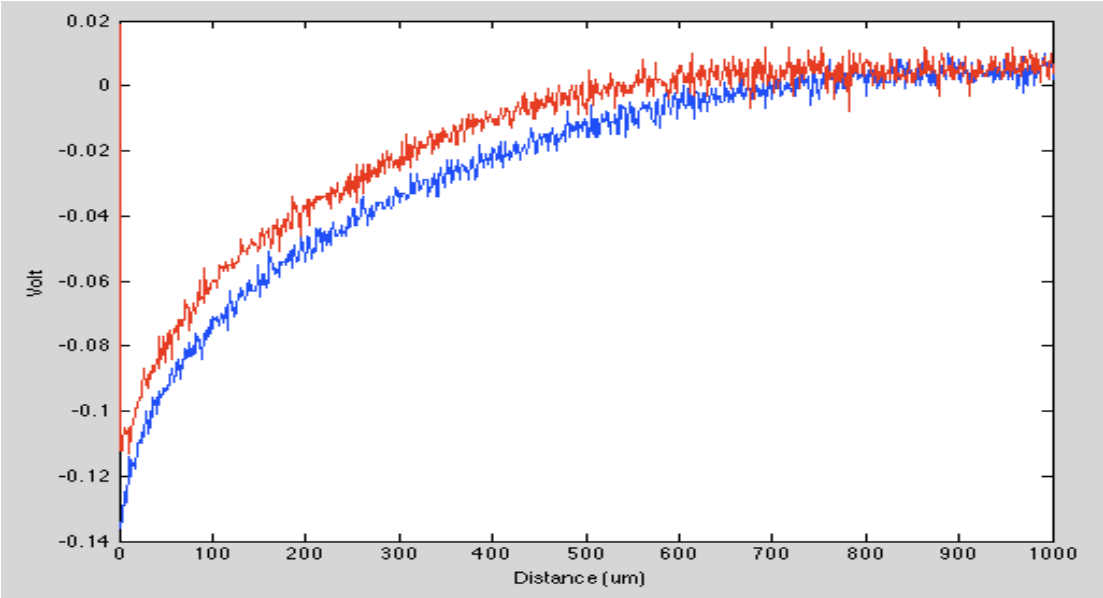

Figure 2.2. Potential profile as a function of distance from the Nafion surface. Blue line: probe electrode moved away from the Nafion surface. Red line: probe electrode moved towards the Nafion surface.

Potentials were plotted as a function of distance from the Nafion surface (Fig. 2.2), and it was clearly observed that the maximum potential ensued at when the probe electrode was on the Nafion surface (distance zero).

The typical I-V curve of single pair 3M KCl micropipette electrodes is shown in Fig. 2.3. The starting potential at distance zero could vary due to the distance between electrode tip and Nafion surface. In order to avoid damaging the electrode tip, the tip was usually placed few microns above the Nafion surface. The best we could control the starting point could vary up to 5 µm.

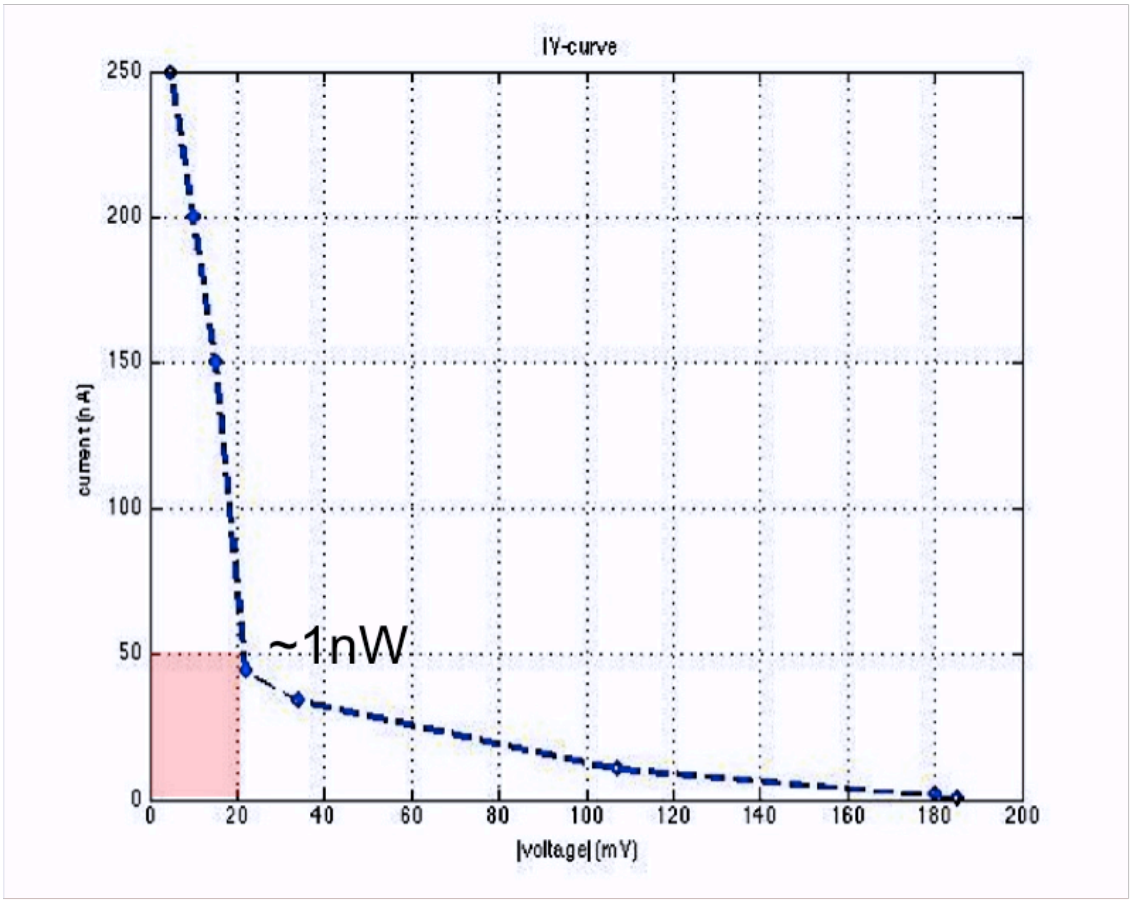

Figure 2.3. Typical IV curve obtained from the use of a single pair 3M KCl micropipette electrodes. The diameter of the electrode tip is 1µm, the maximum power output is about 1 nanoWatts.

From the I-V curve (Fig. 2.3), it can be easily seen that the maximum power output of a 1µm diameter electrode is about 1 nanoWatt. Pilot studies conducted earlier in Pollack lab have shown that infrared radiant energy could dramatically increase the size of interfacial water zone by up to 5 times [2]. Therefore, it is a reasonable assumption that water/interfacial water is merely a medium that can transfer infrared energy from an ambient environment to electricity.

2.2.2 *Multiple Pairs of Micropipette Electrodes*

One of the main challenges of energy harvesting from interfacial water at this stage is to demonstrate its scalability. We set up a proof of concept experiment to show this.

Two sets of 3M KCl micropipette electrode systems (as Fig. 2.1(A)) were set up independently. We used external circuitry to connect these two setups in series or parallel, and then measured the voltage and current of the connected system. It was rationalized that if each setup behaved like an individual energy source, we should be able to observe increase in current when they were connected in parallel and increase in voltage when they were connected in series.

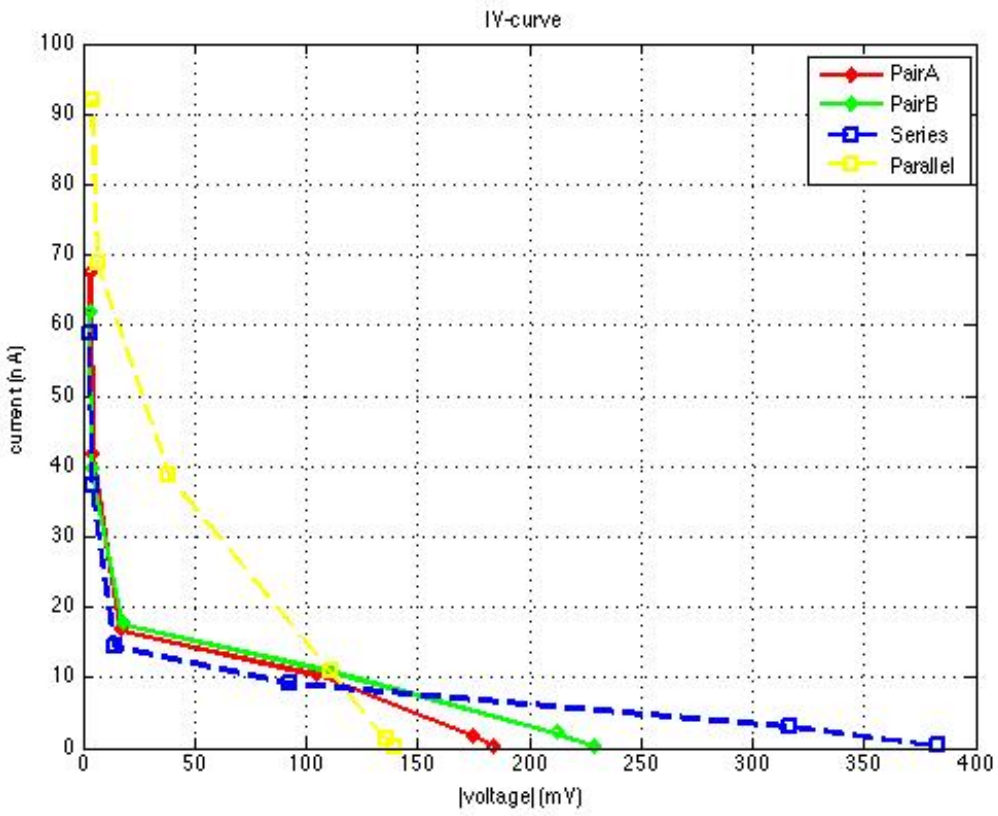

Figure 2.4. The I-V curve obtained from the use of two pairs of 3M KCl micropipette electrodes in series and parallel.

From Fig. 2.4, we can see that the maximum voltage (380 mV) observed after being connected in series was very close to the sum up of the maximum voltage from the two individual pairs (180 mV and 230 mV). The increase in maximum current (92 nA) under a parallel configuration was also increased dramatically as expected; despite being 48 mV less than the sum up of the maximum current from the two individual pairs (62 mV and 68 mV). Thus, the micropipette electrode system appeared to be very promising for its ability to scale up the harvesting of energy.

2.3 MICROFABRICATED ELECTRODE ARRAY SYSTEM

With the success of multiple pairs of micropipette electrodes, we then investigated alternative approaches to further scale up the power output. Conceptually, the more pairs of electrodes we place between the interfacial water and bulk water, the more power we can generate. Depending on the voltage and current requirement for certain applications, we can either connect the multiple pairs of electrodes in series or in parallel or a combination of series and parallel. However, within just one body of water, we can only have the electrodes placed in parallel. Placing the electrodes in series in the same body of water causes internal short circuit between electrodes. In other words, in order to have the electrodes placed in series, we need to have a physically separated bath of water.

It seems a reasonable approach to use the Microelectromechanical System (MEMS) for the electrode array design to achieve higher power output, better efficiency, and compact size. The previous studied micropipette electrode is basically a sharp needle with Ag/AgCl and filled with 3M KCl. In order to mimic our successful electrode design, our goal was to fabricate a micro-needle array with similar construction as the micropipette electrode.

While advances in microneedle design research in the field of biomedical engineering are limited, recent investigations led by Mansoor et al on hollow out-of-plane polymer microneedles

prepared by solvent casting seem to be the most [18] promising for our energy harvesting purpose.

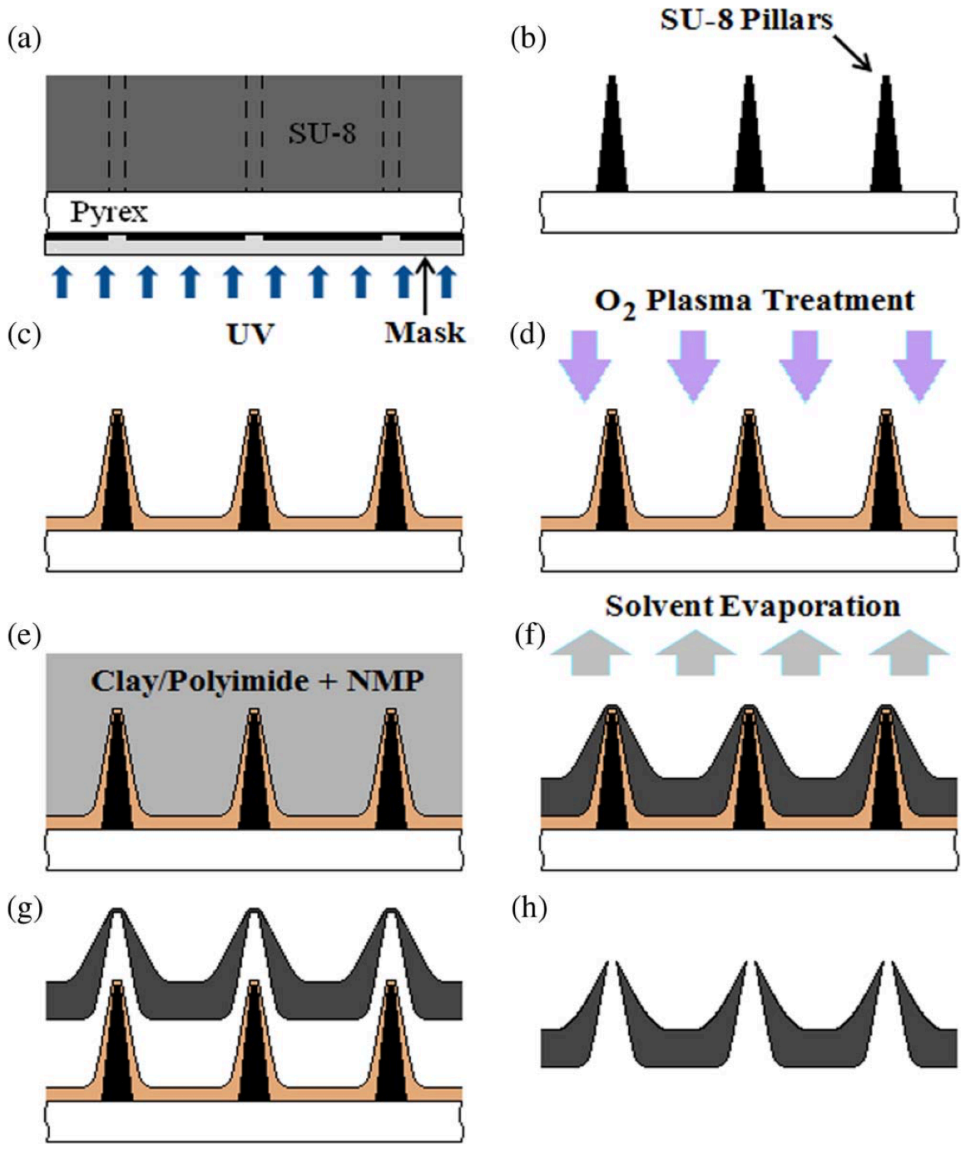

Figure 2.5. Fabrication process using solvent casting for hollow-out-of-plane polymer microneedles, (a) and (b) fabrication of pillars from SU-8, (c) PDMS depo- sition, (d) O_2 plasma treatment of the mold, (e) deposition of a clay/polyimide suspension in NMP, (f) Evaporation of NMP, (g) removing of the microneedle array from the mold, and (h) opening of the microneedle tips. [18]

The fabrication of this microneedle array can be separated into two parts. First, making the reusable SU-8 pillars mold. Second, evaporating the solvent clay/polyimide suspension on the mold to form the microneedle array. The major advantages of this microneedle design (Fig. 2.5) are the inexpensive fabrication and potentially high yield since the mold can be reused over time. However, after some experimentation, we realized that the intrinsic fragility and uneven height of microneedles would be a major concern for our application.

Therefore, we decided to use robust metal conductor as our electrode material. Furthermore, to avoid any oxidation or reduction reaction with water, we chose to use either platinum or gold as the metal. Fig. 2.6 shows the two different designs for the microelectrode array chip. The main difference being that the right design includes electrode plating at the end of the process allowing the metal to extend above the surface of SiO_2 insulator.

Figure 2.6. Simplified diagram for the two different designs of microelectrode array.

In addition to scaling up the power output, the goal was to optimize the density/number of electrodes and the size of the electrode tips as well. While the number of electrodes varied from 1 to 1000, the size was subsequently fabricated from 3 to 20 microns in diameter keeping the same size of electrode array area (2cm*2cm). Fig. 2.7 shows the top view of the electrode array. We only immersed the 2cm by 2cm electrode area in water and left the contact window in the air for connection to an external circuit. This microfabricated electrode array serves as the anode microelectrode array. We sandwiched this anode microelectrode array with Nafion membrane by clamping them together with customized Teflon clamp and have another pure either gold or platinum sheet placed remotely from Nafion as the cathode.

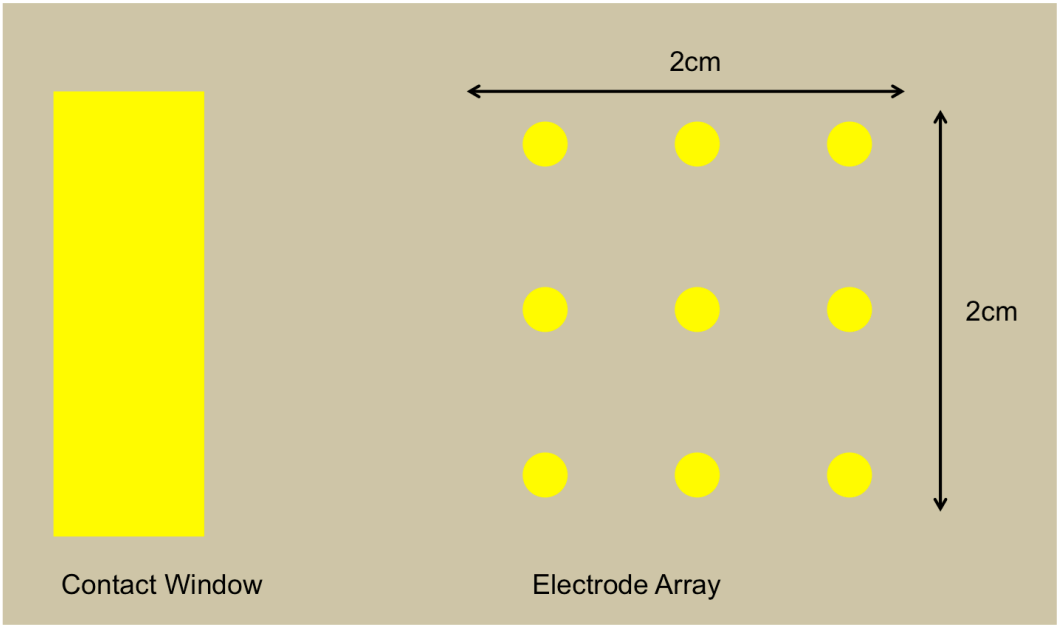

Figure 2.7. The top view of microelectrode array chip. The 2 cm by 2cm area of electrode array will be immersed in water and clamped with Nafion membrane. The contact window is designed to stand above water for connecting to the external circuit.

Unfortunately, the results were not what we expected. Not only was the open circuit voltage unstable, but also the short circuit current seemed unrelated to the size of electrode tip and the number of electrodes within the microelectrode array. It was truly puzzling.

Gradually, we began to understand. The main architectural difference between the microelectrode array and the micropipette electrode is the spacing. In other words, not only is the space between electrodes on the x-y plane important, but also the space in the z-plane between Nafion and electrodes is also crucial for harvesting energy from interfacial water. When we sandwiched the microelectrode array chip with the Nafion membrane, we practically left no space for the interfacial water to be formed and hence failed to get expected results. However, one important lesson was learned. We should raise the vertical height of the anode electrodes, so there is space for the interfacial water be formed properly and the consequential net negative charge of the structured interfacial water would allow us to extract electricity from it. While not

conclusive, the minimum height could be anywhere between 200 μm to 1mm. Because the average size of structured interfacial water is around 200 μm, and the minimum water height we have tested is 1 mm.

2.4 3D PRINTED ELECTRODE ARRAY

Learning from our experience with the microelectrode array system, we realized that the height of the anode electrodes is important in order to have space for the interfacial water to form. Without interfacial water, we lose the medium to convert ambient light energy into electrical charge separation; therefore we can't extract energy from such system anymore.

It is challenging to fabricate microelectrode array that has uniform vertical height over 200 microns. Moreover, the intrinsic fragility of the thin tall microelectrodes is a potential problem for eventual practical application. Nevertheless, we believed the microfabrication technology might still be our best bet to achieve high efficiency and compact size of our prototype device. But in order to move forward to scale up the power at this initial stage, we knew that we needed to find an alternative way for our prototype design.

2.4.1 *Design of 3D Printed Electrode Array*

Advances in the rapidly improving 3D printing technology beginning few decades ago, the solution became clear. The fast prototyping ability of 3D printing with affordable material cost caught our attention. Among the four main 3D printing techniques — stereolithography, selective laser sintering, PolyJet, and thermoplastic extrusion — we chose the PolyJet for its high resolution and multiple materials design freedom. In our designs, we used Stratasys Objet260 printer, which provides 42 microns resolution on the xy-plane and 16 microns on the z-axis. However, in order to get smooth finishing, the minimum size of design features was close to 300 microns.

There are two parts in the 3D printing design (Fig. 2.8). The top is the electrode array. It is one hundred pairs of hollow miniature tubes, both long (10mm) and short (5mm). The long tubes are designed to be placed right on top of the hydrophilic membrane, Nafion, which lay on the floor of the bottom water reservoir. They act as anodes. The short tubes are 5mm away from the hydrophilic membrane surface. They act as cathodes. All tubes have 1mm diameter inner tube size and 1mm wall thickness.

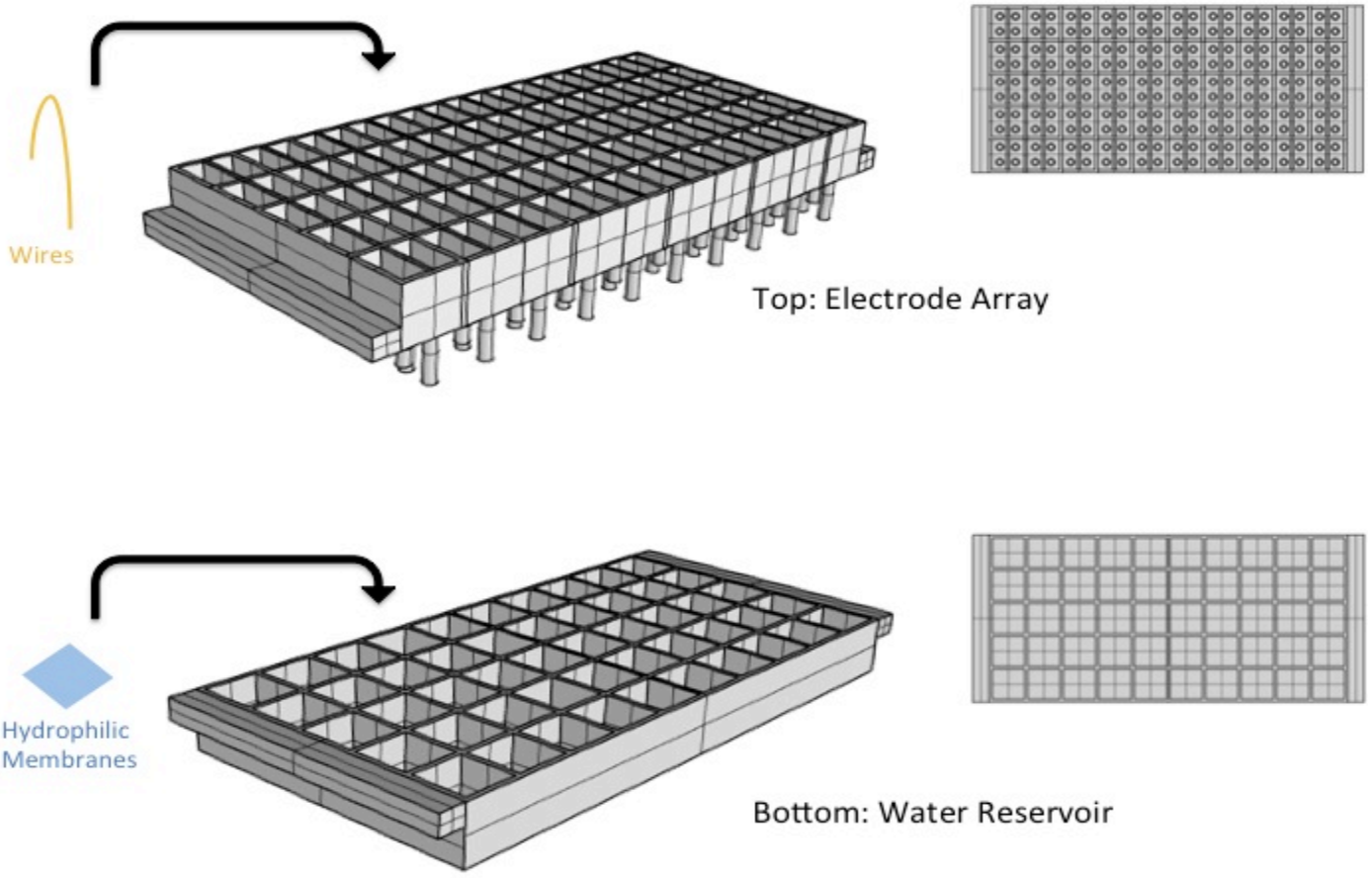

Figure 2.8. Design for the 3D printed electrode array system. The bottom tray consists of fifty separated water reservoir cells in response to the `fifty cells with two pairs of electrode in each cell as the top electrode array.

A complete pair of electrodes includes one long and one short tube, simply a pair of anode and cathode. There are total fifty cells in our top electrode array, and each cell has two pairs of electrodes designed to be connected in parallel. The bottom part has fifty separated water reservoir cells in response to the top electrode array. Each water reservoir cell is 10mm by 10mm by 10mm. The overall size of the 3D printed microelectrode array is 110mm by 56mm by 22mm. It is similar to the size of a smart phone but about double the thickness.

Along with the 3D printed electrode array, we manually place a piece of Nafion 117 perfluorinated membrane at the floor of each bottom reservoir. Silver wires (99% pure) were treated in commercially available bleach for 30 minutes to form Ag/AgCl. Then the Ag/AgCl wires were also manually plugged into the anodes and cathodes, and connected in the series fashion between cells. Within each cell, there are two pairs of electrode were designed to connect in parallel.

2.4.2 *Hydrogel Filling*

The original idea was to integrate 3D printing technology with the existing successful system, micropipette electrode. The fundamental configuration of the micropipette electrode is a fine open tip glass needle filled with 3M KCl and connected with Ag/AgCl metal electrode at the

end. The reason why KCl is the most popular electrolyte in micropipette electrode is the very similar ion mobility of potassium and chlorine. However, prior to starting the 3D printed electrode array design, we already noticed that with the available minimum feature size around 300 microns for 3D printing, there would be a serious issue of the KCl leaking from the electrodes.

This was resolved by searching for a filling material that would prevent the rapid leakage of the KCl electrolyte. .Agarose was the first choice. In biology, agarose gel is often used for gel

electrophoresis in biochemistry and molecular biology. Agarose gel is cheap, easy to make, nonhazardous, and more importantly it is conductive.

Therefore, we tested a range of gels prepared from agarose with concentrations ranging from 1% to 5%. Typically, the agar powder was well mixed with deionized water, then boiled gently and allowed to cool, whereby a gel was formed. However, it was observed that concentrations of agarose greater than 2% were very hard to inject in the 3D printed tube electrodes simply because the warm agarose solution would start forming a gel inside the injecting tools even before filling the tube.

Other modifications included replacing the deionized water used to make the agarose gel with KCl solution to not only increase the conductivity but also to have the proper electrolyte gel for the Ag/AgCl electrode that immersed in the agarose gel for normal function. Indeed, it was discovered that the open circuit potential of this electrode system was related to the KCl concentration used for the agarose gel. Generally speaking, 1M KCl provides the highest open circuit potential at about 100mV to 150mV, which is close to what we usually obtain from the micropipette electrode. With increasing KCl concentration, the agarose gel begins to dissolve in water after a few hours and /or forms cracks easily when placed in the water reservoir. These studies conclusively decided the use of 2% agarose power in 1M KCL solution for the agarose gel.

As depicted in Fig. 2.9, we can see the open circuit potential was increased when two pairs of electrodes were connected in series; similarly, the short circuit current was increased dramatically when two pairs of electrodes were connected in parallel. While these increases on the maximum potential and current were obvious they were clearly not linear. This may be due to the imperfection of each pair electrode. It's much like when connecting a new and an old battery in parallel, the new one starts charging the old one, resulting in lower short circuit current. On the other hand, the nonlinear increase of open circuit voltage while connecting in series was due to the high internal resistance, or Thevinin equivalent resistance, of the electrode system. We will address this issue more in depth in the next section.

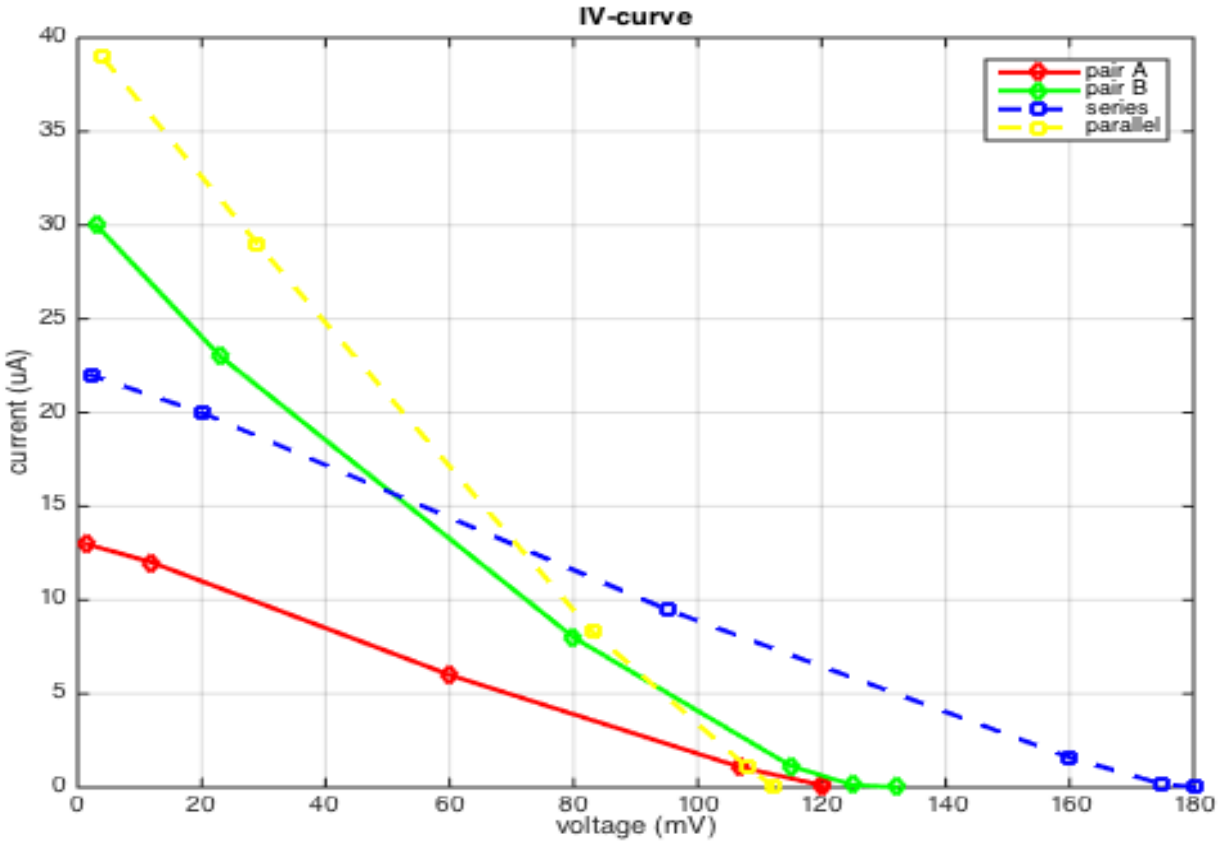

Figure 2.9. The I-V curve obtained from the use of two pairs of 3D printed electrodes with 1M KCl, 2% agarose gel and Ag/AgCl.

Preparation of electrodes: after manually placing the 0.5 mm Ag/AgCl wire in the 1mm wide tube, the bottom opening was sealed with parafilm and finally injected with the agarose electrolyte filling to prevent electrolyte leakage. Once the filling gel solidified, the parafilm was removed. . While acceptable, the imperfections and inconsistency in the functioning and performance of these electrodes resulted mainly from the manual process of inserting and aligning the Ag/AgCl wire at the bottom and center of the tube and the agarose gel. (See Fig. 2.9 between pair A and pair B electrodes).

Another issue we encountered was from the agarose gel filling. The agarose gel broke down slowly after immersion in water for a long time. Typically, we observed the agarose gel started cracking and slightly dissolved in water after a couple hours of immersion in water. Therefore, we then started searching for more durable and conductive hydrogel to replace agarose gel.

After researching the alternatives, we found that zwitterionic gels appeared to be a good replacement for the agarose gel. Not only is the zwitterionic gel chemically bonded with cross-linker which yields better durability, but also the possible engineering process to provide higher conductivity compare to agarose gel.

Pioneering work on zwitterionic hydrogel was carried out on cross-linked HEMA hydrogel by Wichterle and Lim in 1960 [19]. Since then, biomaterial scientists have been fascinated by the biocompatible, durable, and super hydrophilic zwitterionic gel [20], [21] for biomedical applications. In our research purpose, we wanted to use the zwitterionic gel to replace the agarose filling in the 3D printed electrode system. Moreover, with further research, we believe there is a chance to integrate the filling hydrogel and the interfacial water initiated hydrophilic membrane by using just zwitterionic gel. However, this has not been the main focus for now.

We tried a few combinations of popular zwitterionic monomers and cross-linkers. The monomers that we had tested included Carboxybetaine Acryamide (CBAA), Carboxybetaine Methacylate (CBMA), and Sulfobetaine Methacrylate (SBMA); the tested cross-linkers included Ethylene Glycol (EG), Methylenebisacrylamide (MBAA). The only initiator we used was Benacure®1173, so the hydrogel was cured by ultraviolet (UV) light.

Once the gel forms, it is usually kept in deionized water for further hydration. But we kept the gel in 3M KCl to have the gel soaked up the proper electrolyte. The Fig. 2.10 shows the procedures of preparing the zwitterionic hydrogel. It’s basically mixing all the materials at the beginning and had everything well dissolved, and then injected the pre-cure hydrogel, in liquid phase, into the tube electrode. Finally, the gel was cured under the exposure of UV light.

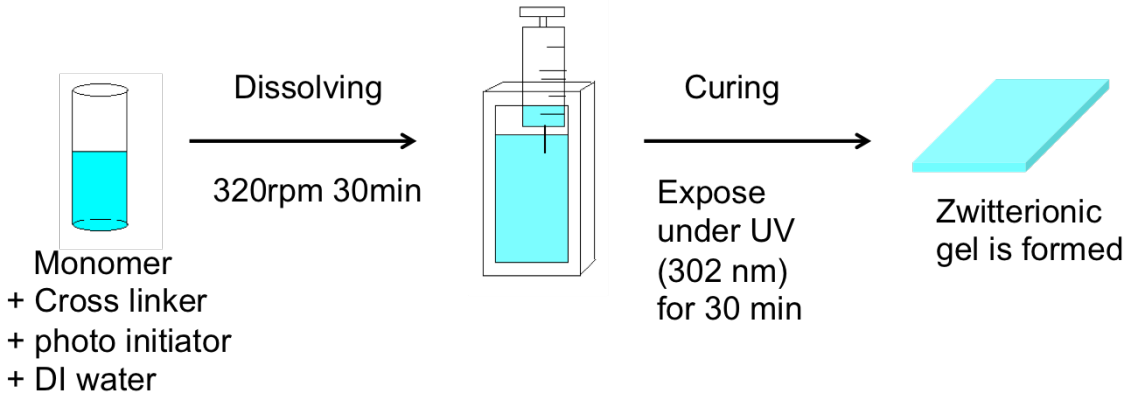

Figure 2.10. Step-wise procedures for making the zwitterionic hydrogel.

In addition to cross-pairing the chosen monomers and the cross-linkers, different concentrations of monomer and cross-linker for the hydrogel were experimented. Pilot tests revealed a yield of an open circuit potential of about 60 to 80 mV with the 3D printed electrode system configuration using a 33% SBMA monomer with MBAA and a 1% EG cross-linker.

The zwitterionic hydrogel works much like the agarose gel. However, we were still not satisfied with the small improvement of the mechanical strength of the zwitterionic hydrogel, not to mention that the open circuit potential was considerably smaller (about 20% to 30%) than using agarose gel. So we started to try the double-network structure hydrogel [22], which seems promising to provide very strong mechanical properties. The core idea of the double-network hydrogel is to induce double-network structure with more than one monomer, Scientists even tried to utilize the double-network hydrogel for making artificial articular cartilage.

Furthermore, in order to improve the durability of the filling hydrogel, and also achieve a high open circuit potential, the possibility of engineering more negative ions in the monomer for the anode electrode and positive ions in the monomer for the cathode electrode, appeared likely in increasing the potential difference between the anode and cathode and production of additional power. Therefore, we chose the 2-Acrylamido-2-Methylpropane Sulfonic Acid (AMPS) to pair with SBMA to form the double-network hydrogel for the anode electrodes. For the cathode electrodes, we used (3-Acrylamidopropyl) trimethylammonium chloride and SBMA as the

double-network hydrogel filling. In both cases, MBAA was used as the cross-linker, 5% for the anode hydrogel, and 7% for the cathode hydrogel. The chosen concentrations of cross-linkers were able to achieve the formation of a highly durable hydrogel while compromising elasticity and rigidity. The initiator used in both cases was Benacure®1173. The chemical structure of chosen monomers and the cross-linker are shown in Fig 2.11.

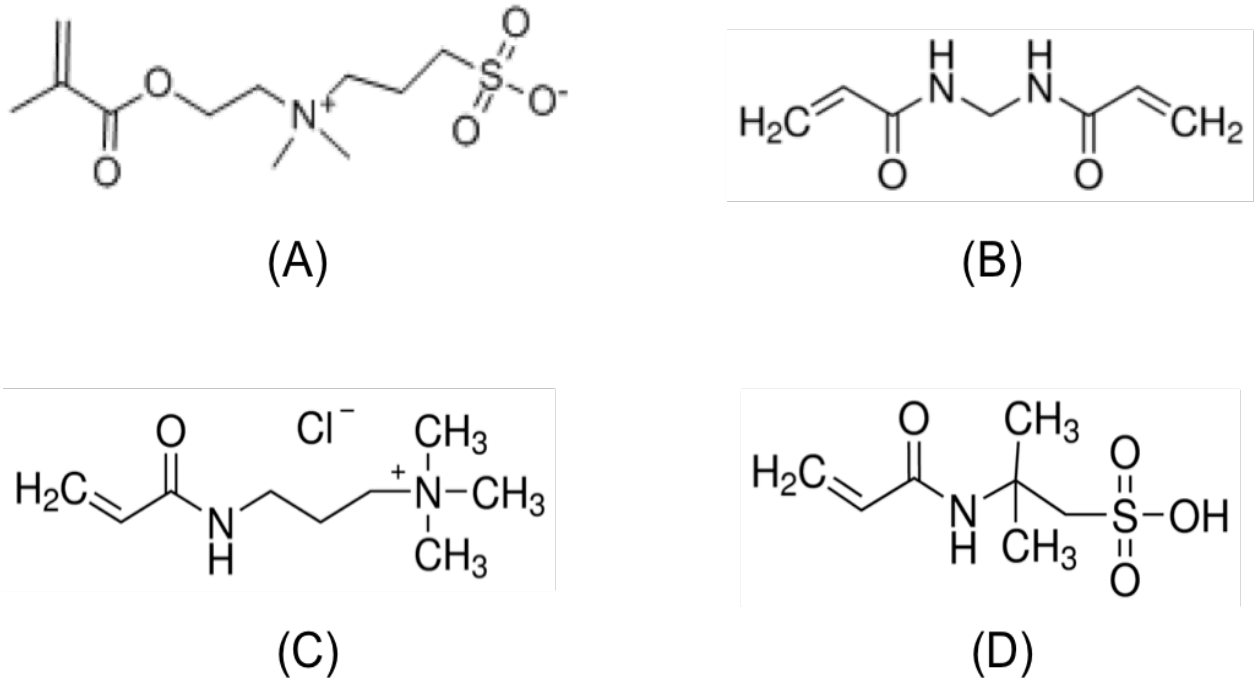

Figure 2.11. The chemical structures of selected monomers and cross-linker. (A) Sulfobetaine Methacrylate (SBMA). (B) Methylenebisacrylamide (MBAA). (C) (3-Acrylamidopropyl) trimethylammonium chloride. (D) 2-Acrylamido-2-Methylpropane Sulfonic Acid (AMPS).

Results obtained from the two-pair electrode tests are shown in Fig. 2.11. It is clear that when the two pairs of electrodes were placed in series, the open circuit potential added up nicely from each pair; and the same was true for the short circuit current. We then moved on to use these double-network structure hydrogels on the whole 3D printed electrode array for our ultimate test.

With a total fifty cells in the electrode array, and each cell containing two pairs of electrodes connected in parallel. The fifty cells would be connected in series externally. In other words, one hundred pairs of electrodes, each two pairs were connected in parallel and fifty two-pairs were connected in series.

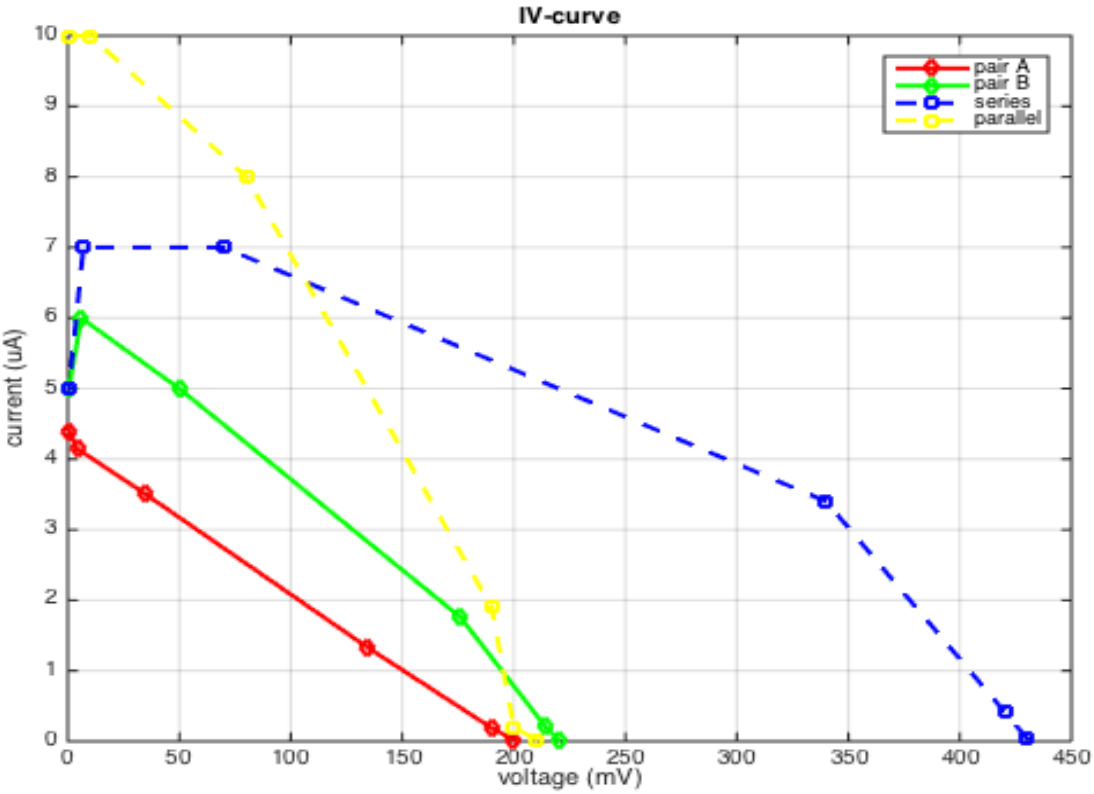

Figure 2.12. The I-V curve obtained from the use of two pairs of 3D printed electrode with double-network structure hydrogels and Ag/AgCl.

The final 3D printed electrode system test is shown in Fig. 2.13. With 50 cells in series, this 3D printed electrode array can deliver maximum about 9V to 10V. Since each cell contains two pairs of electrodes connected in parallel, the maximum current output is about 10 μA. In order to reach the maximum power output of this total 100 pairs electrode array, the electrodes should be all connected in parallel — or at least most of them. From the previous I-V curves we can see that, for a single pair electrode, the maximum power output happens when the load resistance is 1 to

10 KΩ. To increase the voltage or current when the load resistance is about 1 to 10 KΩ, connecting electrodes in parallel serves the purpose better than in series. However, this 3D printed electrode was designed to have 50 cells connected in series and each cell has two pairs electrodes connected in parallel. It is really challenging to connect all electrodes in parallel. Since all Ag/AgCl wires are half immersed in the hydrogel, trying to make connections between wires can easily cause the wire come out or loose from the filling gel. The best we could achieve with the current design was 300mV under 10KΩ load resistor with 50 pairs of electrodes, which provided close to 100μW.

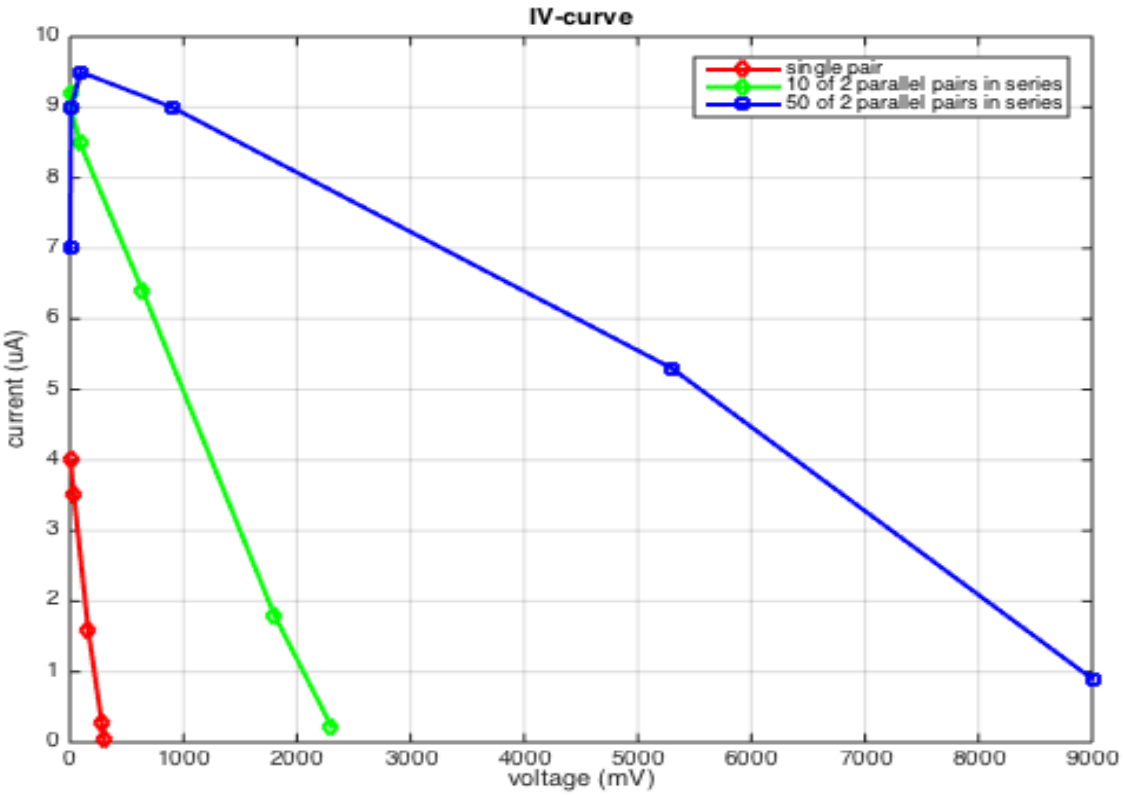

Figure 2.13. I-V curve of 1, 20, and 100 pairs of 3D printed electrode with double-network structure hydrogel and Ag/AgCl. Red line represents the single pair. Green line represents the total 20 pairs, each two pairs in parallel, and 10 of two pairs are connected in series. Blue line represents the total 100 pairs, each two pairs connect in parallel, and 50 of two pairs are connected in series.

2.5 DISCUSSION

2.5.1 *Basic Circuit Model*

To model the energy harvesting from interfacial water device, we use the basic Thevenin equivalent circuit model, which is shown in Fig. 2.14. In the circuit simulation model, we simplified the device to have only passive resistance. Our goal is to use this simplified simulation model to help us to further understand and to improve our next device design.

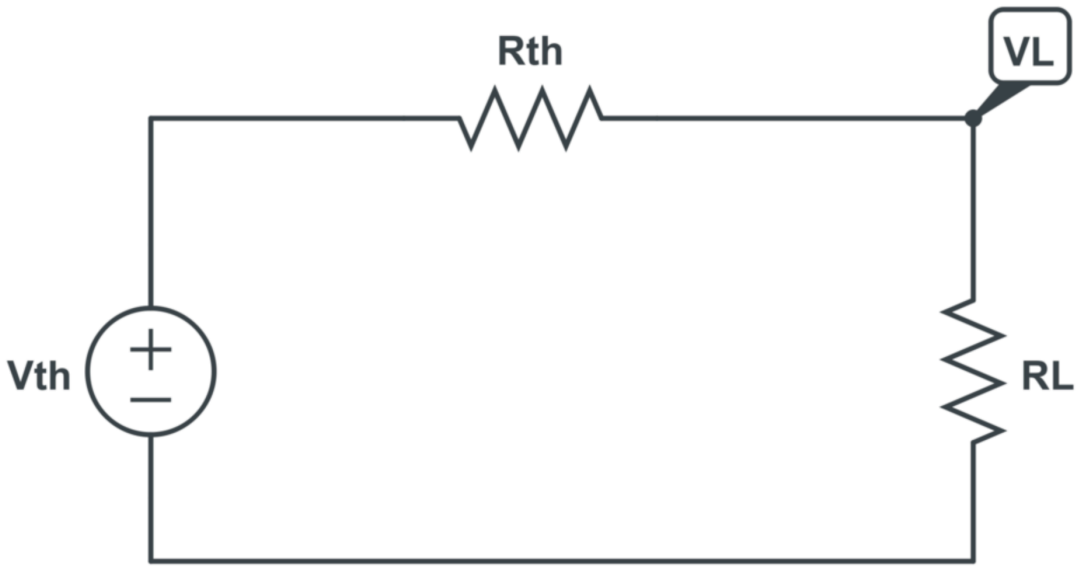

Figure 2.14. Thevenin equivalent circuit model for the energy harvesting from interfacial water device. V_{th} is the Thevenin equivalent voltage. R_{th} is the Thevenin equivalent resistance. R_L is the load resistance and V_L is the voltage across load.

The Thevenin equivalent voltage is the same as the open circuit voltage of our device, the load resistance was chosen by us, and the load voltage is measured across the load resistor. Therefore, the Thevenin equivalent resistance can be calculated using equation (2.3)

$$V_{th} = I_L \times R_{th} + V_L \quad (2.1)$$

$$I_L = {}^{V_L}/_{R_L} \quad (2.2)$$

$$R_{th} = \frac{(V_{th} - V_L) \times R_L}{V_L} \quad (2.3)$$

In the proposed micropipette electrode system, R_{th} is about 1 to 3 MΩ. As an energy source, this MΩ R_{th} is huge and non-practical for any application, causing a big voltage drop internally. In other words, the energy is not used by the load resistor but rather consumed internally as waste internally. The main reason why the R_{th} is so big for the micropipette electrode is the physical size of the electrode tip, which is usually about one micron in diameter or smaller. However, there is a way we can get around this low energy transfer-efficiency challenge.

Imagine if we have many pairs of electrode connected in parallel, then the total equivalent R_{th} would decrease at a rate proportional to the number of pairs in parallel. So the new equivalent R_{th}' will be R_{th}/n if there are n pairs of electrodes connected in parallel (Fig. 2.15). The math is easy to derive from Ohm's law.

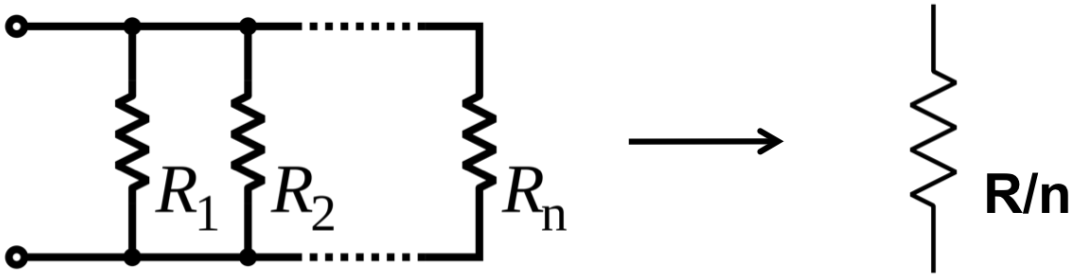

Figure 2.15. If R_1=R_2...=R_n, then the R_{eq}=R/n.

Moreover, enlarging the size of electrode was found to have a similar effect as having multiple pairs connected in parallel and reduced the equivalent R_{th} dramatically. Current studies, however, depict a less linear effect than when actual pair up with multiple pairs of electrodes. Electrodes with ten times larger size does not reduce the equivalent R_{th} by a factor of ten. This is because the influence elements are not only the size of electrode tip but also the contact area of the Ag/AgCl wire with KCl and the effective size of the structured interfacial water.

Nevertheless, the nonlinear factor could be improved by modifying the configuration of electrode design. Assuming that we can have the equivalent R_{th} inversely proportional to the size of electrode. Then to have the R_{th} less than 10 Ω, we need the electrode with size of about 3 mm^2, which is fairly practical and appealing compact size. Even though we haven't achieved result like this, we know what is the goal to set for.

In the current 3D printed electrode system, the electrode tip opening is 1 mm^2, and the equivalent Thevenin resistance is about 30 KΩ. While this resistance is indeed 100 times smaller than that of the micropipette electrode, studies need to be conducted to investigate how to drop the Rth to be at least less than 100 Ω.

2.5.2 *Controls*

Current investigations on energy harvesting from interfacial water have frequently been questioned by the following two most common questions- "Is this a potato battery?" and "So it's a concentration cell?" .

2.5.2.1 Potato Battery

The potato battery is a simple battery that often made for educational purposes. It demonstrates the Galvanic cell battery in an easy and inexpensive way. A galvanic cell is an electrochemical

cell that provides electricity from the chemical redox reactions happening within the cell. Usually, people use zinc as the anode and copper as the cathode.

Each metal has its own standard electrode potential, which is determined by comparing to the platinum hydrogen standard reference electrode. Because of the different standard electrode potentials of different metals, electrical potentials can be created between two metals. Therefore, with proper electrolyte in the cell, the current would be generated spontaneously. For the potato or lemon battery, using a zinc nail and a copper penny provide good anode and cathode materials. Even though the juice electrolyte is not ideal, it can still deliver enough power to light an LED if multiple pairs are connected in series.

However, these galvanic cell types of battery only work when the anode and cathode are made of different metal material with different standard electrode potentials. Without an electrical potential difference exists between the anode and cathode, there would be no current generated, and therefore, no production of energy. In the energy harvesting from interfacial water device, identical materials have always been used for both anode and cathode of the electrode system, thereby sufficiently distinguishing these two types of devices.

2.5.2.2 Concentration Cell

From the Nernst equation, equation (2.4), we know that there are two ways to produce electricity in an electrochemical cell. The first one as described above, is based on the use of two different metals for constructing the anode and cathode so the different standard electrode potentials between the anode and cathode drive the electromotive force to generate electricity. The second one is based on the difference in the ion concentration in the electrolyte between anode and cathode, which could also induce electromotive force within an electrochemical cell.

The Nernst equation:

$$E = E_{cell} + \frac{RT}{zF} lnQ \qquad (2.4)$$

where E is the cell potential at the temperature of interest, E_{cell} is the standard cell potential, R represents the universal gas constant, T represents the temperature, z represents the number of moles of electrons transferred in the cell reaction, F represents the Faraday constant, and Q represents the reaction quotient.

Because we use identical Ag/AgCl wires for both anode and cathode, the standard cell potential Ecell is zero. The half-cell reactions at the anode and cathode are shown in equation 2.5 and 2.6.

Half-cell reaction at anode:

$$Ag + Cl^- \rightarrow AgCl + e^- \qquad (2.5)$$

Half-cell reaction at cathode:

$$AgCl + e^- \rightarrow Ag + Cl^- \qquad (2.6)$$

There is only one electron involved in each half-cell reaction, so z is one. The reaction quotient is determined by the ratio of concentration difference of Cl^- between anode and cathode. It is well known that during the fabrication process, the manufacturers immerse Nafion in hydrochloric acid (HCl) solution to activate the membrane. Even though there is usually a DI-water cleaning step right after the acid treatment, it is possible that some chlorine lingers on the Nafion. Thus, the question that remains to be investigated next is if the small amount of chlorine that persisted on the Nafion membrane is able to cause the 100 to 200 mV potential difference that is usually observed from such electrode system.

The short answer to the question is “No”. We have two reasons. First, according to the Nernst equation, the chlorine ion concentration difference between the anode and cathode will need to be 10 to 100 times so as to generate the 100 to 200 mV cell potential. The 3M KCl we used as electrolyte was already very high, close to over saturated. It is unlikely that the hidden chlorine

ions in Nafion can cause such huge difference in concentration on top of the preexisting chlorine ions from the electrolyte. Second, Nafion is not the only hydrophilic membrane we use for energy harvesting. While it remains as the main material, because its stable performance and so far it provides the highest power output. However, other chlorine free hydrophilic membrane such as cellulose acetate can also provide constant power, which was tested by our electrode system.

It is clear that our energy harvesting system is not a chlorine induced concentration cell. However, the reason that we can use deionized water as the medium to convert ambient electromagnetic energy into electricity is the interfacial structure water. As the consequence of such structure, the charge separation formed. There are fewer protons in the about 200 microns size interfacial region. Water, H_2O, is original electrically neutral. So it's not hard to figure out that there are more protons in the bulk water region.

Moreover, the main reason we used Ag/AgCl as our electrode material is because of its supreme stability. But the major draw back of using Ag/AgCl to convert ionic current into electric current is the device longevity. To solve this, we had tried using inert electrodes like platinum, palladium, glassy carbon and etc. We noticed that using inert electrodes to replace Ag/AgCl could cause significant current drop in our system. It is due to the less active chemical properties of such "inert" materials. One way to get around this issue is to add additive electrolyte ions such as iodide and triiodide, ferricyanide and ferrocyanide, and etc. to a liquid portion of the electrode structure, to a hydrogel portion of the electrode structure, and/or to the water itself. So the electrolyte ions can help transferring electron from/to the inert electrodes. In other words, higher current output can be achieved. It's also been confirmed from our preliminary experiments and calculation that the additive electrolyte ions cannot cause the potential difference we observed in our electrode system just like the case of chlorine we mentioned above.

Chapter 3. EFFECT OF ATOMOSPHERIC IONS ON INTERFACIAL WATER

3.1 MATERIALS AND METHOD

The preparation of hydrophilic membrane (Nafion) and deionized water are the same as Chapter 2. As for the probe electrode, we only use the micropipette electrode whose fabrication process mentioned earlier in chapter 2.

A high voltage generator (ES30P-5W, Gamma High Voltage Research) was used to create the coronal discharge, which produced positive air ions.

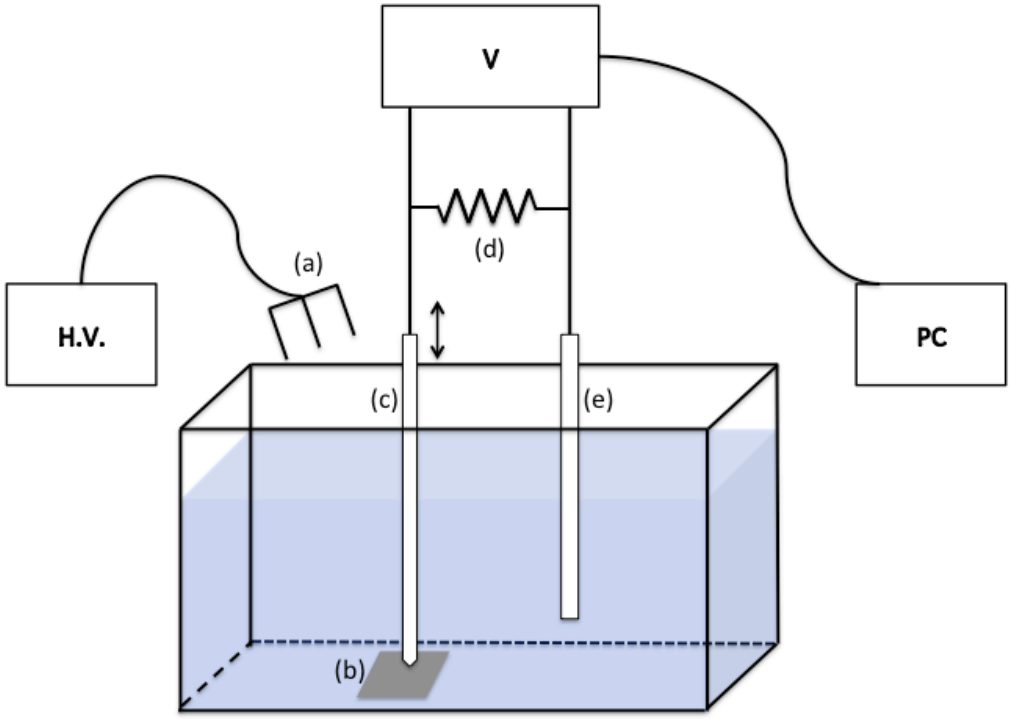

Figure 3.1. Experimental setup. (a) The discharge electrodes connected to the high voltage (H.V.) generator. (b) Nafion membrane. (c) The probing microelectrode. (d) 1,000 MΩ passive resistor placed parallel with the electrometer. (e) The reference electrode.

The experimental setup is shown in Fig. 3.1 Electrical potentials were measured with an electrometer (Model 6512, Keithley) and recorded on the computer through a data acquisition device (USB-6009, National Instruments). A flexible reference electrode (WPI) was placed remotely from the interfacial region. A 1,000 MΩ passive resistor was placed in parallel with the electrometer terminals to keep the load resistance constant and to facilitate readout of the current extracted from interfacial water. The resistor also helped to reduce ambient electromagnetic noise.

We first positioned the probing microelectrode immediately above and just touching the Nafion surface to obtain the most stable and highest magnitude electrical potential readout. The reference electrode was placed remotely. Before turning on the high voltage source, we measured the potential profile as a function of distance from the Nafion surface. The probing microelectrode was moved away from the Nafion surface by increments of 1.25 μm until it reached 1 mm from the Nafion surface. The electrical potential was recorded at each pause. After the potential profile measurement was completed, the system automatically brought the probing microelectrode back to the Nafion surface. The data thus collected provides reference information to be compared with the experimental results obtained in the presence of positive air ions.

High-voltage discharge was used to produce air ions. We turned up the voltage from 0 kV to 10 kV at 1 kV intervals. The discharge electrodes were located 3 cm above the water surface. Potentials as a function of increasing voltage were measured by the probing electrode and recorded simultaneously. Then we maintained the high voltage at 10 kV for 10 minutes and measured the potential profile once again. We set the 10 kV limit because at about 10.5 to 11kV, the discharge electrodes began generating electric arcs which interfered with all nearby electronic equipment and made measurements inconsistent thereafter.

The probing microelectrode was brought back to the Nafion surface automatically after the second potential profile measurement was completed. Then, we reversed the procedure, turning down the high voltage gradually back to zero and recording the potential between the two

electrodes at 1 kV intervals. At the end, the potential profile was recorded again to check the reversibility of the air-ion effect.

Control experiments were conducted to clarify whether the effect on interfacial water was indeed from air ions or from electrical polarization due to the high voltage discharge electrodes or from the ozone generated during the coronal discharge. To test for electrical polarization, we used two identical reference electrodes in deionized water without the Nafion sheet. The two electrodes were placed side by side equally close to the high voltage discharge electrodes horizontally, at different heights in water. To test for the ozone, we used a copper metal mesh to cover the top of the chamber. Since the metal mesh sheet was grounded, no air ions could reach the water, while the electrically neutral ozone could still do so.

3.2 RESULTS

Electrical potential measurements on the water-Nafion interface have been carried out many times with consistent results. When the probing electrode is very close to the Nafion surface, sometimes, even touching, and the reference electrode placed remotely, the magnitude of the potential difference between the two electrodes is the highest. It can range from -100 to -200 mV. Most often, its value is approximately -120 mV.

With the methods described in Materials and Methods, we measured the potential profile vs. distance from the Nafion surface as well as the highest potential before, during, and after applying the high voltage. Before turning on the high voltage supply, we obtained results similar to those found earlier. A representative potential profile is shown in Fig. 3.2 (A).

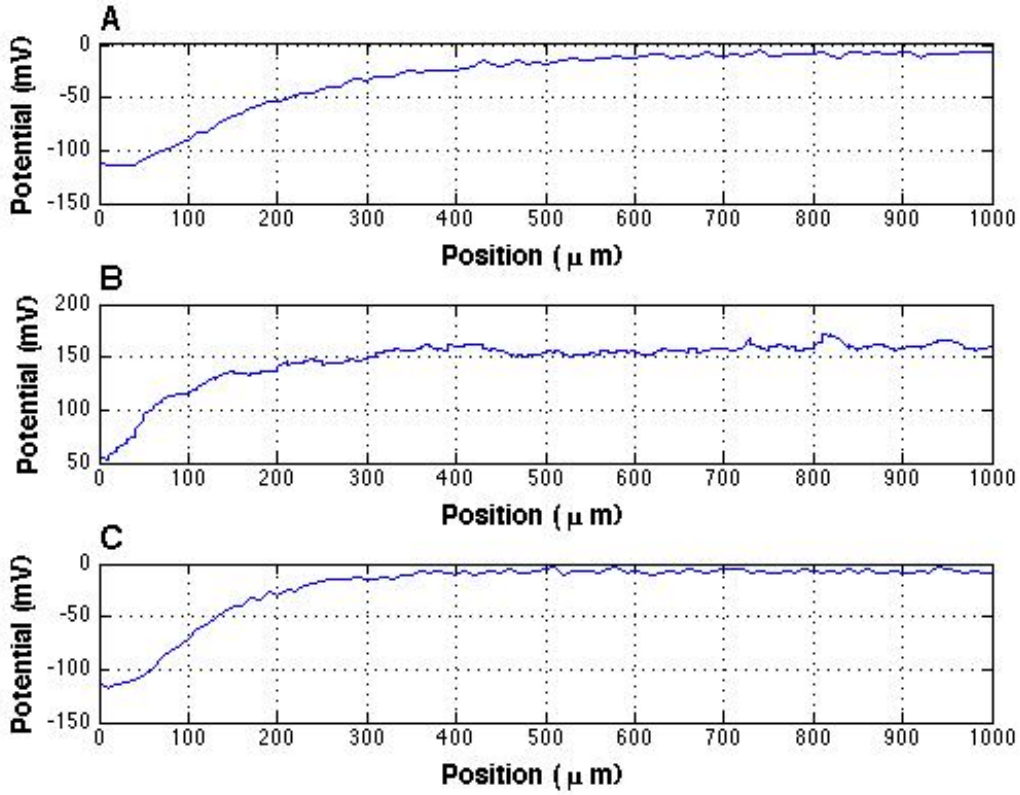

Figure 3.2. Potential profile as a function of distance from the Nafion surface, to a distance of 1 mm. (A) Measured before turning on the high voltage power supply. (B) Measured ten minutes after turning the high voltage power supply to 10 kV. (C) Measured after the high voltage power supply was turned off.

Next, the high voltage power supply was turned on and the potential between the two electrodes was recorded while the voltage was increased in 1 kV increments. This probe electrode remained at a fixed position in the water near the Nafion surface. Fig. 3.3 (blue line) shows that the electrical potential remained the same (less than 3% change) at all voltages below 8 kV. However, starting from around 9 kV, the electrical properties of interfacial water began changing noticeably. At the end, even the polarity changed from negative to positive.

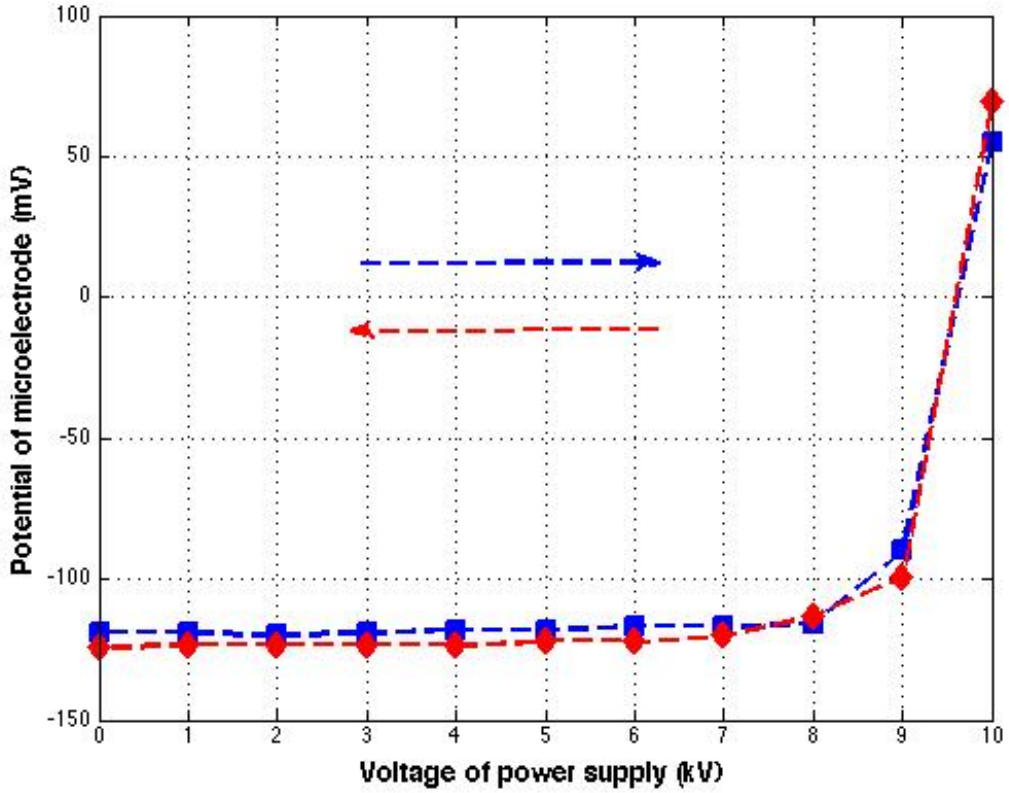

Figure 3.3. The potential difference between the probe and reference electrodes recorded at progressively increasing (blue)/ decreasing (red) increments of 1 kV.

Fig. 3.2 (B) depicts the potential profile that was obtained ten minutes after the voltage of power supply reached 10 kV. As can be observed, the potential profile already shifted in the positive zone while the microelectrode was probing in the interfacial water region. This implies the positive air ions can transfer through to the interfacial water, thus changes its electrical properties.

The altered electrical properties of the interfacial water were fully reversible. Fig. 3.3 (red line) shows the result obtained during successive reductions of the high voltage. The results fit in nicely with those obtained during the voltage upturn (blue line), except that the order was reversed. The polarity returned to negative between 10 and 9 kV, with no obvious change seen

from 8 to 0 kV. Upon reaching zero, the final potential profile measurement showed a return to the values obtained before turning on the high voltage supply (Fig. 3.2 (C)).

Shutting down the high voltage supply directly from 10 kV produced similar results: the potential between electrodes promptly jumped back approximately to the initial value within just a few seconds. This was an interesting finding, since positive ions dissolved in water are not expected to disappear so fast. However, previous work from this laboratory has shown that interfacial water forms rapidly, implying that the return to negative potential may be due to the rapid re-building of negatively charged interfacial water.

Next we investigated if the altered electrical properties genuinely arose from the air ions, or from some other features such as polarization of water or ozone produced from coronal discharge.

According to standard electrical theory, any positive charge placed above a body of water (a dielectric material) should induce negative charge on top of the water, while the bottom becomes more positive. However, the air ion effect did the opposite: it made the water more positive on top than the bottom (Fig. 3.2 (B)). Apparently, positive charge from the high voltage source must have entered the water.

To check that conclusion, we removed the Nafion and placed two identical reference electrodes in the deionized water. One electrode was kept at mid-height of the chamber, while the other was moved vertically, to the top, middle and bottom. When the high voltage source was turned on, the top of the water was clearly more positive than the bottom.

In order to rule out the influence of ozone produced from coronal discharge as the possible cause of the electrical changes, a grounded copper metal mesh was positioned on top of the chamber to block any charged air ions from entering into the water, while allowing the uncharged ozone to pass through. We then elicited coronal discharge by turning up the voltage to 10 kV, the highest value possible before creating an electric arc. The potential difference between the two electrodes barely changed (less than 3 percent). This observation confirmed that without entry of

the charged ions, the electrical properties of interfacial water would not change, implying that the observed potential changes were indeed caused by the positive ions and not by artifacts such as ozone or other byproducts of coronal discharge.

A question is whether naturally occurring changes of atmospheric charge have similar effects on interfacial water. During our earlier experiments on the electrical properties of interfacial water, we noticed small amplitude periodic variations of electrical potential. On investigating, we found that those variations were related to the airflow from the laboratory air conditioner: we used an acoustic microphone placed at the air conditioner outlet, and confirmed that the higher the airflow, the louder the noise.

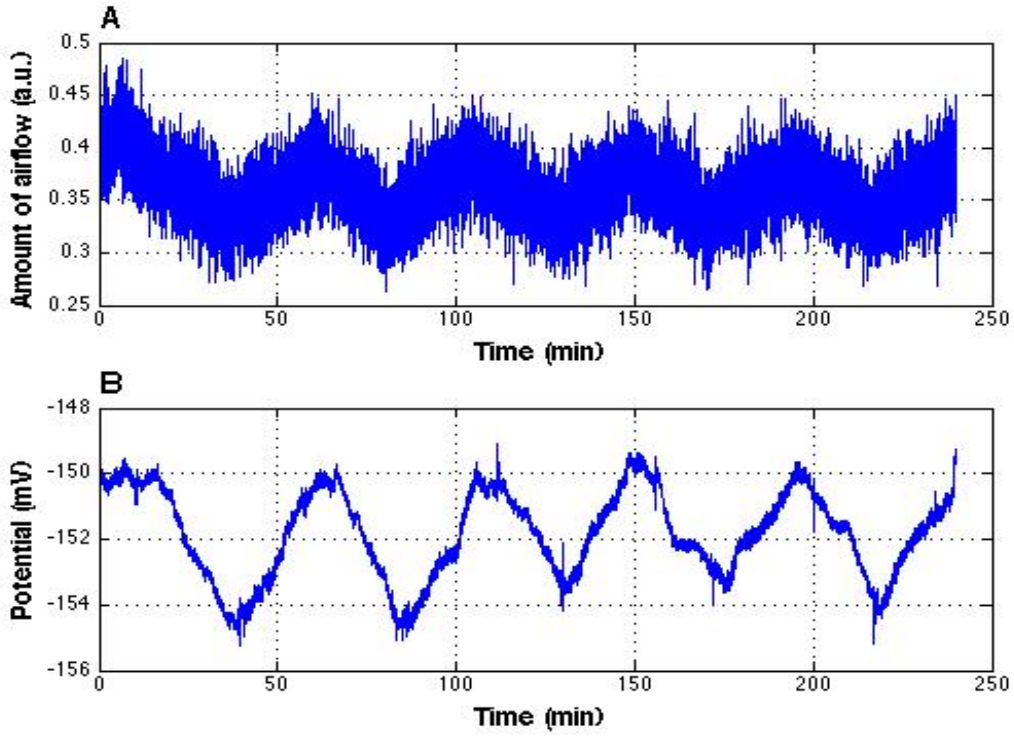

Figure 3.4. Simultaneous recordings of the airflow signal from the air conditioner (A) and the electric potential of interfacial water (B). Note that the peaks and valleys of both the signals are in alignment.

We therefore recorded the airflow over an extended period (4 hours) while simultaneously measuring the electrical potential of interfacial water. We confirmed an excellent alignment of the periodic change in potential (about 4 mV in amplitude) with the airflow from the air conditioner (Fig. 3.4). The period was approximately 50 minutes. Throughout the experiment, the measured change of water temperature was less than one degree Celsius.

These observations may be explained by the fact that air conditioners are sources of charged air. When air is forced to flow through pipes and filters, it becomes positively charged due to friction. In fact, air is the most positive substance of the triboelectric series[23]. The air's positive charge can help explain how the airflow from the air conditioner can impact the electrical features of interfacial water.

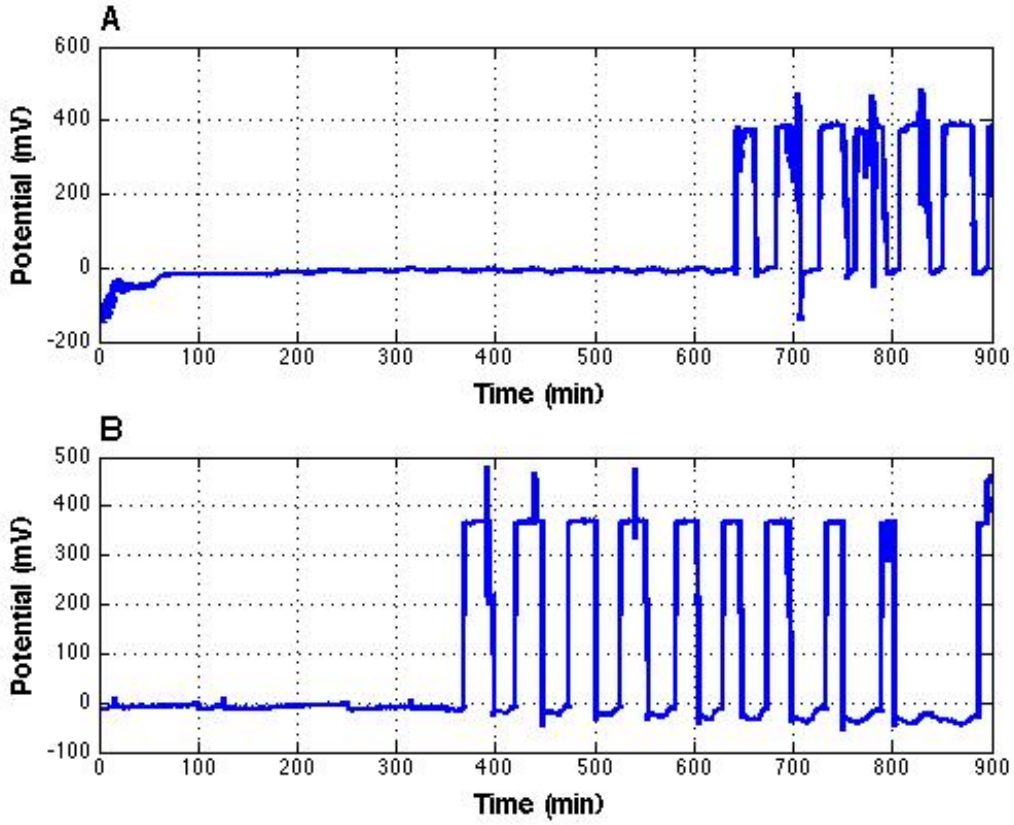

Figure 3.5. Unusual dramatic change in the overnight potential recording of interfacial water. The first 15 hours (A) were interspersed by an 8 hours gap before the next 15 hours recording (B).

While the effects of the laboratory air conditioner were generally modest, one occasion produced a rather astonishing observation. Fig. 3.5 shows an overnight potential recording with the same set-up as Fig. 6 but without the high voltage power supply. The amplitude change was over 400 mV, and the period was about 50 minutes, the same as the air conditioner (compare Fig. 3.4). Because the period is similar, we believe the "skyscraper" oscillations arose from the positively charged air ions coming from the air conditioner.

While there were small periodic changes (similar to those of Fig. 3.4) during the first ten hours of recording, suddenly at about 10.5 hours, the potential dramatically changed to a high positive value close to 400 mV (Fig. 3.5 (A)). This kind of threshold effect fits the experimental results described earlier in this paper. We later recorded the potential of interfacial water for another 15 hours, without changing the experimental setup, and observed similar results (Fig. 3.5 (B)). The one missing skyscraper oscillation near the end of the recording implied that the air conditioner might not have supplied sufficient positive air ions for threshold crossing, the same as during early periods in the two recordings.

These observations confirmed our findings that airflow from ordinary air conditioners can appreciably change the electrical properties of interfacial water.

3.3 DISCUSSION

Generally speaking, negative charge is believed to promote good health, whereas positive charge compromises health.[3], [4], [24],[14], [15] Nature provides a reasonably balanced supply of air ions; however more negative ions are found at places such as waterfalls and forests[25], which often elicit sensations of well being. The question arises whether these effects are largely psychogenic or whether some physical mechanism exists to explain the effects.

One common denominator of function may be cell water. By volume, our bodies are roughly 2/3 of water, and much of that water is interfacial; i.e., it resides next to some hydrophilic interface

[6]. More recent experimental observations of interfacial water have shown that interfacial water is negatively charged.[1], [26] This negative charge could be reduced by atmospheric positivity and thereby cause adverse health effects. In other words, if this water, along with the proteins it envelops, is vital for function, then compromising the amount of interfacial water could impair function.

The experimental results were consistent with this hypothesis. In the experiments involving high voltage, a threshold voltage was required to produce enough air ions to have appreciable impact on the interfacial water. When the discharge electrodes were placed 3 cm from the water surface, the threshold voltage required to produce enough air ions was approximately 8 kV. From this result we infer that positive ions in the air may change concentration appreciably without having adverse health effects. However, beyond a threshold concentration, the ill effects of positive charge may become appreciable — even wiping out the negativity of interfacial water and replacing it with the many positive ions in the water.

The rapid rebuilding of interfacial water once the positive ions were removed is consistent with earlier results. Interfacial water builds rapidly. Once the inhibiting positive ions are removed, the structure can easily and quickly rebuild. In terms of health impact, this suggests that restoration of function can occur rapidly once the positive air ions are removed. This phenomenon can potentially explain the “refreshing” sensation that people often feel when stepping out of a crowded room with positive ions from exhalation, and into fresh air.

We obtained similar results with positive ions produced from an air conditioner. When the conditions are right, enough air ions could be produced to change the electrical properties of the interfacial water. The example of dramatically changed electrical potential indicated that the structure of interfacial water could be completed destroyed by positive air ions, perhaps explaining the serious consequences people can sometimes suffer in sufficiently foul air. More generally, this result may explain the natural craving to escape from air-conditioned environments and into natural air.

Chapter 4. CONCLUSION AND FUTURE WORKS

There are two main interesting phenomena as an outcome of structured interfacial water. One is the solute free exclusion zone property, and the other is the charge separation. In my work, I focus on the possible applications base on the charge separation property.

From an occasional event, we found the intriguing relationship between the atmospheric ions and interfacial water. With further study, we realized that to date, there is still no conclusive conclusion on the biological effects of air ions. We had proved the effect of atmospheric ions on interfacial water experimentally. This provides a new point of view for the centuries long debate on the air ions and health.

There is plenty of research ongoing worldwide for the relationship between interfacial water and health. With more and more clues and evidence unveiled, we expect to have the missing dots connected in the near future and eventually understand the mechanism of how air ions affect biological system.

On the other hand, we investigated tremendous amount of time to develop the energy-harvesting device to extract the charge separation energy from interfacial water. Humanity has been always hungry for more energy, and especially renewable energy. Fossil fuel had brought us a never-seen-before technology boost; however, it also caused many serious environmental damages to us. We are proud to be part of the community that working on solving or at least helping this global energy crisis.

Even the energy harvesting from interfacial water technology is still at its infant stage, we know we have been moving forward step by step every single day. To make this technology appropriate for practical use, our mission is to

BIBLIOGRAPHY

[1] J.-M. Zheng, W.-C. Chin, E. Khijniak, E. Khijniak Jr., and G. H. Pollack, "Surfaces and interfacial water: Evidence that hydrophilic surfaces have long-range impact," *Advances in Colloid and Interface Science*, vol. 127, no. 1, pp. 19–27, Nov. 2006.

[2] B. Chai, H. Yoo, and G. H. Pollack, "Effect of Radiant Energy on Near-Surface Water," *J. Phys. Chem. B*, vol. 113, no. 42, pp. 13953–13958, Oct. 2009.

[3] J. M. Charry and F. B. Hawkinshire, "Effects of atmospheric electricity on some substrates of disordered social behavior.," vol. 41, no. 1, pp. 185–197, 1981.

[4] A. R. Sovijärvi, S. Rosset, J. Hyvärinen, A. Franssila, G. Graeffe, and M. Lehtimäki, "Effect of air ionization on heart rate and perceived exertion during a bicycle exercise test. A double-blind cross-over study.," vol. 41, no. 4, pp. 285–291, Aug. 1979.

[5] J. HENNIKER, "The Depth of the Surface Zone of a Liquid," *Rev Mod Phys*, vol. 21, no. 2, pp. 322–341, 1949.

[6] *Cells, gels and the engines of life*. Ebner and Sons Publishers, 2001.

[7] K. A. Mauritz and R. B. Moore, "State of Understanding Nafion," pp. 1–52, Jul. 2004.

[8] B. Franklin, "A Letter from Mr. Franklin to Mr. Peter Collinson, F. R. S. concerning the Effects of Lightning," *Philosophical Transactions of the Royal Society of London*, vol. 47, no. 0, pp. 289–291, Jan. 1751.

[9] Dalibard, T.F. Letter to Academy of Science. 1749.

[10] A. P. Krueger, "The biological effects of air ions," *Int J Biometeorol*, vol. 29, no. 3, pp. 205–206, Sep. 1985.

[11] G. Phillips, G. J. Harris, and M. W. Jones, "Effect of air ions on bacterial aerosols," *Int J Biometeorol*, vol. 8, no. 1, pp. 27–37, Mar. 1964.

[12] A. P. Krueger, "Studies on the Effects of Gaseous Ions on Plant Growth: I. The influence of positive and negative air ions on the growth of Avena sativa," *The Journal of General Physiology*, vol. 45, no. 5, pp. 879–895, May 1962.

[13] M. Diamond, J. Connor, E. Orenberg, M. Bissell, M. Yost, and A. Krueger, "Environmental influences on serotonin and cyclic nucleotides in rat cerebral cortex," *Science*, vol. 210, no. 4470, pp. 652–654, Nov. 1980.

[14] Y. Palti, E. De Nour, and A. Abrahamov, "THE EFFECT OF ATMOSPHERIC IONS ON THE RESPIRATORY SYSTEM OF INFANTS," *Pediatrics*, 1966.

[15] S. Kotaka and A. P. Krueger, "Effects of Air Ions on Microorganisms and Other Biological Materials," *Critical Reviews in Microbiology*, vol. 6, no. 2, pp. 109–150, Jan. 1978.

[16] L. B. Loeb, *Electrical Coronas*. Univ of California Press, 1965.

[17] B. Sulbarán, G. Toriz, G. G. Allan, G. H. Pollack, and E. Delgado, "The dynamic development of exclusion zones on cellulosic surfaces," *Cellulose*, vol. 21, no. 3, pp. 1143–1148, Jan. 2014.

[18] I. Mansoor, U. O. Hafeli, and B. Stoeber, "Hollow Out-of-Plane Polymer Microneedles Made by Solvent Casting for Transdermal Drug Delivery," *J. Microelectromech. Syst.*, vol. 21, no. 1, pp. 44–52.

[19] O. Wichterle and D. Lím, "Hydrophilic Gels for Biological Use," *Nature*, vol. 185, no. 4, pp. 117–118, Jan. 1960.

[20] F. Nederberg, J. Watanabe, K. Ishihara, J. Hilborn, and T. Bowden, “Organo Hydrogel Hybrids. Formation of Reservoirs for Protein Delivery,” *Biomacromolecules*, vol. 6, no. 6, pp. 3088–3094, Nov. 2005.

[21] A. S. Hoffman, “Advanced Drug Delivery Reviews,” *Advanced Drug Delivery Reviews*, vol. 64, no. S, pp. 18–23, Dec. 2012.

[22] J. P. Gong, Y. Katsuyama, T. Kurokawa, and Y. Osada, “Double-Network Hydrogels with Extremely High Mechanical Strength,” *Adv. Mater.*, vol. 15, no. 14, pp. 1155–1158, Jul. 2003.

[23] Adams, C.K. *Nature's Electricity*; TAB Books: Blue Ridge Summit, PA, USA, 1987.

[24] C. H. Bachman, R. D. McDonald, and P. J. Lorenz, “Some physiological effects of measured air ions,” *Int J Biometeorol*, vol. 9, no. 2, pp. 127–139, Jun. 1965.

[25] Luts, Parts, Laakso, Hirsikko, Gronholm, Kulmala, “Some air electricity phenomena caused by waterfalls: Correlative study of the spectra,” *Atmos Res*, vol. 91, no. 2, pp. 9–9, Feb. 2009.

[26] Pollack, G.H. *The Fourth Phase of Water: Beyond Solid, Liquid, and Vapor*; Ebner and Sons Publishers: Seattle, WA, USA, 2013.

VITA **SUMMER 2015**

CHIEN-CHANG KUNG

5317 7th Ave NE 206-407-8945
Seattle WA 98105 ckung@uw.edu

EDUCATION

- **Bachelor of Science - National Chiao Tung University**
  Major: Wireless Communication Engineering June 2007

- **Master of Science – University of Washington**
  Major: Electrical Engineering Dec 2012

- **Technology Entrepreneurship Certification – University of Washington** March 2015

- **Dual Ph.D. in Electrical Engineering & Nanotechnology – University of Washington**
  Research Topic: Energy Harvesting from Water Sep 2009 – June 2015

EXPERIENCES

Research Assistant in the international Atacama Large Millimeter Array (ALMA) project
Sep 2006 – Sep 2007

- Simulated practical roughness surface in a multi-layer structure by EM software.
- Designed a model to authenticate the reflectivity of the rough aluminum surface is high enough to be a reflector of Atacama Large Millimeter Array.

Communications Corporal in the R.O.C. Army Oct 2007 – Sep 2008

- Managed and maintained various communication equipment in the R.O.C. Army, including both wired and wireless communication devices.

Lab Manager in the Pollack lab under UW Bioengineering Department Sep 2012 – Present

- Managed the lab major operations. Organized and mentored the undergraduate researches.

Research Associate in the Disney Research Lab, Pittsburgh Jun 2014 – Sep 2014

- Designed and developed prototype for cavity resonant mode wireless power system.

Current Projects

Characterizing the molecular structure of interfacial water Jun 2010 – Present

- Developing polarized microscopy platform to determine the birefringence property of interfacial water.

The effect of atmospheric ions on interfacial water Jun 2012 – Dec 2013

- Studying how atmospheric ions could affect interfacial water, whose results might provide new insights into biological effect of air ions.

Energy Harvesting from Water Jun 2011 – Present

- Characterizing electrical properties of interfacial water.
- Designing and developing microelectrode array system by using MEMS/NEMS fabrication process.
- Using 3D printing technology for rapid prototyping minimum viable product for energy harvesting from water

SKILLS

● Programming: C, C++, MATLAB, Labview
● Software: HFSS, IE3D, CST, Pspice, Mathematica, AutoCAD, Photoshop, Adobe Illustrator
● Hardware: Analog Circuit Design, Micro/Nano Fabrication, Electrochemistry, 3D Printing Technology, Microwave Electronics, Biological Wet Bench (ex, PCR, Cell Culture), Microfluidic Device, Various Microscopies

Areas of Interest

Energy Harvesting, Renewable Energy, Wearable Devices, and Biomedical Devices

Publication

● Effect of atmospheric ions on interfacial water, 1st author. *Entropy*, 2014
● Novel Water Based Renewable Energy Technology, 1st author. in progress

EXTRACURRICULAR ACTIVITIES

● Volunteer and Member, National Water Life Saving Association. Sep 2000 – present
● Mobile Phone Antenna Contest, Industrial Development Bureau, Ministry of Economic Affairs, Taiwan Mar – Sep 2007
● Scholarship and Poster in Water conference, Vermont, USA Oct 2010
(Title: The Influence of Microwave Frequency Electromagnetic Wave on Interfacial Water)
● Scholarship and Poster in Water conference, Vermont, USA Oct 2011
(Title: Can Water Behave Like a Battery?)
● Scholarship and Poster in Water conference, Vermont, USA Oct 2012
(Title: Energy Harvesting from Water)
● Scholarship of Electric Universe conference, Albuquerque, USA Jan 2013
(Title: Energy Harvesting from Water)
● Highest Prototype Funding - $5000 USD Jan 2013
(University of Washington Environmental Innovation Challenge)

- The Most Innovative Project Award — Jan 2013
  (University of Washington Science & Technology Showcase)
- Scholarship and Poster in Water conference, Sofia, Bulgaria — Oct 2013
  (Title: Effect of atmospheric ions on interfacial water)
- The Best Communicator Prize in University of Washington Sci & Tech Showcase — Feb 2014
  (Title: Energy Harvesting from Water)
- The Best Poster Award in Electrical Energy Industrial Consortium, Seattle, USA — Apr 2014
  (Title: Energy Harvesting from Water)
- The Best Poster Award in University of Washington MoLE Showcase — May 2014
  (Title: Energy Harvesting from Water)
- Scholarship and Poster in IEEE Power and Energy Society, DC, USA — Jul 2014
  (Title: Can Water Behave Like a Battery?)
- The Best Poster Award in Water Conference, Sofia, Bulgaria — Oct 2014
  (Title: Energy Harvesting from Water)
- Invited Speaker in UW Scholar's Studio, Seattle, USA — Jan 2015
  (Title: Water, Light, Electricity)
- Sustainability Project Grand Award - $10,000 USD — Jun 2015
  (University of Washington Campus Sustainability Fund)